Molecular Biology of the Cell
Vol. 21, 1698–1713, May 15, 2010

Keratin 8/18 Modulation of Protein Kinase C-mediated Integrin-dependent Adhesion and Migration of Liver Epithelial Cells

François Bordeleau,* Luc Galarneau,* Stéphane Gilbert, Anne Loranger, and Normand Marceau

Centre de Recherche en Cancérologie and Département de Médecine de l'Université Laval, and Centre de Recherche du Centre Hospitalier Universitaire de Québec (CRCHUQ), Quebec City, QC, Canada G1R 2J6

Submitted May 6, 2009; Revised March 19, 2010; Accepted March 22, 2010
Monitoring Editor: M. Bishr Omary

Keratins are intermediate filament (IF) proteins of epithelial cells, expressed as pairs in a lineage/differentiation manner. Hepatocyte and hepatoma cell IFs are made solely of keratins 8/18 (K8/K18), the hallmark of all simple epithelia. Cell attachment/spreading (adhesion) and migration involve the formation of focal adhesions at sites of integrin interactions with extracellular matrix, actin adaptors such as talin and vinculin, and signaling molecules such as focal adhesion kinase (FAK) and member(s) of the protein kinase C (PKC) family. Here, we identify the novel PKCδ as mediator of the K8/K18 modulation of hepatoma cell adhesion and migration. We also demonstrate a K8/K18-dependent relationship between PKCδ and FAK activation through an integrin/FAK-positive feedback loop, in correlation with a reduced FAK time residency at focal adhesions. Notably, a K8/K18 loss results to a time course modulation of the receptor of activated C-kinase-1, β1-integrin, plectin, PKC, and c-Src complex formation. Although the K8/K18 modulation of hepatocyte adhesion also occurs through a PKC mediation, these differentiated epithelial cells exhibit minimal migrating ability, in link with marked differences in protein partner content and distribution. Together, these results uncover a key regulatory function for K8/K18 IFs in the PKC-mediated integrin/FAK-dependent adhesion and migration of simple epithelial cells.

INTRODUCTION

Keratins (Ks), the intermediate filament (IF) proteins of epithelial cells, constitute the largest family of cytoskeletal proteins and are grouped into type I (K9-28) and type II (K1-K8 and K71-K80) subfamilies (Schweizer *et al*., 2006). Keratin IFs are obligate heteropolymers that include at least one type I and one type II keratin, and they are coordinately expressed as specific pairs in a cell lineage and differentiation manner. For example, keratinocytes in the epidermis (squamous epithelium) express the K5/K14 pair in the basal layer and the K1/K10 pair in the upper layer upon terminal differentiation (Coulombe and Wong, 2004). Cells of simple (single-layered) epithelia, like those involved in the renewal of the intestinal epithelium, express K7, K8, K18, K19, K20, and K23 as different pair partners, with K8/K18 being a pair common to all of them (Marceau *et al*., 2004; Omary *et al*., 2009). Notably, K8 and K18 are the ancestral genes for the multiple specialized type II and type I keratin classes, respectively, and constitute the first keratin genes expressed in the embryo (Oshima *et al*., 1996). Even though hepatocytes progressively differentiate during development and undergo maturation at the postnatal stage, they maintain K8 and K18 only (Marceau *et al*., 2001). Like all IF proteins, K8 and K18 consist of a central a-helical (rod) domain flanked by N- and C-terminal globular "head" and "tail" domains (Fuchs and Weber, 1994; Herrmann *et al*., 2004). Although IF protein assembly into IFs takes place through heterodimerization of rod domains (Coulombe and Omary, 2002), the head and tail domains contribute to most of the structural heterogeneity of IF proteins among tissues, and they serve regulatory and functional purposes (Coulombe and Omary, 2002; Omary *et al*., 2006). In this regard, K8/K18 head and tail domains contain phosphorylation motifs at serine sites that are recognized by mitogen-activated protein (MAP) kinases and also by protein kinase C (PKC) (Ridge *et al*., 2005; Ku and Omary, 2006; Omary *et al*., 2006; Sivaramakrishnan *et al*., 2009), and in turn changes in K8/K18 domain phosphorylation status modify their IF dynamics, solubility, and organization (Omary *et al*., 2006). But conversely, K8/K18 IFs act as modulators of kinase and caspase signaling pathways in hepatocytes (Toivola *et al*., 2001; Gilbert *et al*., 2004; Loranger *et al*., 2006; Gilbert *et al*., 2008), a prominent functional trait that is in line with the genetic-based evidence on the multifunctional features of K8/K18 IFs and their contribution to liver disease predisposition (Omary *et al*., 2009). Of particular note, like other IF proteins, K8/K18 seem to largely exert their functions through interactions with associated proteins, such as plectin (Green *et al*., 2005), a cytolinker that also possesses binding sites for actin and microtubule-associated proteins (Rezniczek *et al*., 2004), which makes it a key player in the integration of regulatory and functional cytoskeleton-related events.

A tight control of cell adhesion and migration is crucial for a wide variety of physiological and pathological processes, such as embryogenesis, wound healing, and tumor metas-

This article was published online ahead of print in *MBoC in Press* (http://www.molbiolcell.org/cgi/doi/10.1091/mbc.E09–05–0373) on March 31, 2010.

* These authors contributed equally to this work.

Address correspondence to: Normand Marceau (normand.marceau@crhdq.ulaval.ca).

tasis (Lee and Juliano, 2004). These cellular processes mainly occur through integrins, the heterodimeric (α/β) cell surface receptors that mediate cell–extracellular matrix (ECM) interactions (Geiger *et al*., 2001; Hynes, 2002). Integrin binding to an ECM protein elicits signals that are transduced intracellularly to regulate cell growth, migration, and survival; conversely, integrin engagement is modulated by intracellular signaling cascades leading to changes in attachment and spreading efficiency (Hynes, 2002; Lee and Juliano, 2004). Cell migration actually involves cycles of cell attachment to and detachment from ECM that require the dynamic turnover (assembly and disassembly) of integrin-mediated focal adhesions (FAs) (Caswell *et al*., 2009). In turn, there is evidence indicating that FA disassembly occurs mainly through a caveolin-1 (Cav-1)-regulated mechanism (Goetz *et al*., 2008). Originally identified as a substrate for c-Src (Glenney, 1989), Cav-1 has also been identified as a regulator of Rho/Rho kinase-dependent FA dynamics and tumor cell migration and invasion (Joshi *et al*., 2008). Still, as transmembrane components of FAs, integrins affiliate with ECM via their extracellular domains and associate via their intracellular domains with actin cytoskeleton adaptors such as talin and vinculin, and with signaling molecules such as focal adhesion kinase (FAK), a key partner of c-Src (Mitra and Schlaepfer, 2006; Meng *et al*., 2009). In addition, PKC has been found to play a pivotal role in integrin-mediated signaling (Besson *et al*., 2002). PKC constitutes a 12-isoform family of serine/threonine kinases that have been categorized into conventional PKCs (α, β1, β2, and γ), novel PKCs (δ, ε, υ, τ, ω, and μ), and atypical PKCs (ι and ζ), based on their requirement or not for Ca^{2+} and/or diacylglycerol (DAG), and their differential activation by phorbol 12-myristate 13-acetate (PMA), which acts as an alternative stimulus to DAG (Parker and Murray-Rust, 2004). Depending on cell type, different PKC isoforms are involved in integrin engagement (Laudanna *et al*., 1998; Ng *et al*., 1999), and this occurs through binding to anchoring proteins, such as receptor for activated C-kinase (RACK1), which regulates their localization to specific subcellular compartments (Liliental and Chang, 1998; Chang *et al*., 2002). Of note, RACK1 has been shown to link novel PKC to β1-integrin and to be required for glioma cell adhesion and migration (Besson *et al*., 2002) and to affect keratinocyte migration in a plectin-dependent manner (Osmanagic-Myers *et al*., 2006).

The ability of simple epithelial cells to migrate seems to be linked to cell differentiation status and tissue homeostatic features. For example, the renewal of the epithelium covering the intestine is characterized by stem cell production and differentiation in the crypts, subsequent migration out of the base of the villi and further migration as cohesive sheet of differentiated cells to the tip of the villi where they are shed by anoikis (Crosnier *et al*., 2006). The migrating cells transiently adhere to an ECM, which composition varies differentially along the crypt-villus axis, in an integrin-linked kinase (ILK)-dependent manner (Gagné *et al*., 2010). In glandular epithelia like liver, the hepatocyte differentiation starts in the embryo as foregut endodermal cells migrate into the new ECM environment of the surrounding mesenchyme; already at that time, the liver mass constitutes a well defined structure expressing typical glandular differentiated functions (Lora *et al*., 1998). Although the surrounding matrix remains of particular importance for the maintenance of normal hepatocyte functions at the postnatal stage, variations in ECM deposition are not translated into hepatocyte migration (Lora *et al*., 1998; Gkretsi *et al*., 2007). The development of invasive hepatocellular carcinoma (hepatoma) is associated with the capacity of the cancerous cells to form metastatic nodules in the remaining liver parenchyma through an intricate multiprocess cascade that includes differential cell adhesion, migration and ECM proteolysis (Mizuno *et al*., 2008). Thus, because hepatoma cells, like hepatocytes, express solely the K8/K18 pair (Galarneau *et al*., 2007; Bordeleau *et al*., 2008), the two cell types provide models of choice to address the role of the K8/K18 pair by itself as modulator of simple epithelial cell behavior, including integrin-dependent adhesion and migration. In this regard, we have found recently that K8-knockout mouse hepatocytes and K8-knockdown H4-II-E-C3 (shK8b) rat hepatoma cells exhibit a reduced capacity to spread on fibronectin compared with their K8/K18-containing counterparts, wild-type (WT) hepatocytes and H4ev cells (Galarneau *et al*., 2007). Here, the same liver epithelial cell models were used to address the K8/K18 IF modulation of integrin-dependent adhesion and migration of cancerous versus differentiated simple epithelial cells on fibronectin, in terms of cell adhesion/migration response to PKC activation/inhibition, PKC versus FAK phosphorylation, and interplay between RACK1, integrin and related partners. The results indicate that PKCδ works as a mediator of the K8/K18 modulation of hepatoma cell adhesion and migration, a K8/K18 loss leading to perturbations in PKCδ versus FAK activations, PKC-dependent integrin/FAK feedback loop, and RACK1/β1-integrin/plectin/PKC/c-Src complex formation. Although a comparable K8/K18 modulation of the adhesion occurs through a PKC mediation in hepatocytes, these differentiated epithelial cells exhibit minimal migrating ability on fibronectin, in correlation with marked differences in binding partner content and distribution between the two simple epithelial cell types.

MATERIALS AND METHODS

Reagents

Primary antibodies used were as follows: mouse monoclonal anti-Talin (T3287) and anti-vinculin (V9131; Sigma-Aldrich Canada, Oakville, ON, Canada); mouse monoclonal anti-RACK1 (sc-17754; Santa Cruz Biotechnology, Santa Cruz, CA); mouse immunoglobulin (Ig)M anti-RACK1 (610178), rabbit polyclonal anti-caveolin-1 (610060), mouse monoclonal anti-β1-integrin (610467), anti-PKCα (610107), anti-PKCδ (610397), and anti-FAK (610087; BD Biosciences Pharmingen, Mississauga, ON, Canada); rabbit anti-phospho Y397 FAK (44624G; Invitrogen, Burlington, ON, Canada); mouse monoclonal anti-glyceraldehyde-3-phosphate dehydrogenase (GAPDH) (10R-G109a; Fitzgerald Industries, Concord, MA); mouse monoclonal anti-Src(L4A1) (2110), rabbit polyclonal anti-PKCδ (2058), anti-phospho-PKCδ(Thr-505) (9374), and anti-caveolin-1 (3238; Cell Signaling Technology, Danvers, MA); rabbit polyclonal anti-PKCε (06–991) and anti-ILK (06-550-MN; Millipore, Billerica, MA); Alexa Fluor 488 Armenian hamster IgG anti-mouse/rat β1-integrin (102212; BioLegend, San Diego, CA); and rabbit polyclonal anti-plectin, rat monoclonal anti-mouse K8, and mouse monoclonal anti-rat K8 (Galarneau *et al*., 2007). Secondary antibodies used were as follows: Alexa 488-goat anti-mouse IgG, Alexa 555-goat anti-mouse IgG, and Alexa-594-goat anti-rabbit IgG (Invitrogen, Burlington, ON, Canada); Texas Red-goat anti-mouse IgM (Jackson ImmunoResearch Laboratories, West Grove, PA); and horseradish peroxidase-goat anti-rabbit IgG and anti-mouse IgG (Bio-Can, Mississauga, ON, Canada). Fetal bovine serum (FBS) was purchased from Wisent (Quebec, QC, Canada); green fluorescent protein (GFP)-FAK was kindly obtained from Dr. L. H. Tsai (Harvard Medical School, Boston, MA), GFP-Paxillin was from Dr. K. Jacobson (University of North Carolina, Chapel Hill, NC), and GFP-vinculin was from Dr. B. Geiger (Weizmann Institute of Science, Rehovot, Israel). Empigen BB, Src family inhibitor PP2 and PKC inhibitors bisindolylmaleimide I (BIM) and Gö6976 (Gö) were purchased from Calbiochem (Mississauga, ON, Canada). Small interfering RNA (siRNA) against PKCα (Rn-Prkca-7 HP siRNA [SI03092348]), PKCδ (Rn-Prkcd-5 HP siRNA [SI03055073]), and PKCε (Rn-Prkce-6 HP siRNA [SI03059959]) were purchased from QIAGEN (Mississauga, ON, Canada). All other chemicals were from Sigma-Aldrich Canada.

Hepatocyte Isolation and Culture

Details on the establishment, maintenance, and genotyping of the K8-deficient FVB/N mouse line were reported previously (Marceau *et al*., 2004). The

experiments were performed according to the rules of the Laval University Animal Care Committee. Hepatocytes were isolated according to a version of the two-step collagenase method as described previously (Galarneau *et al*., 2007). The cells were plates on fibronectin-coated 35-mm dishes in DME/F-12 modified medium supplemented with sodium selenite (5 μg/l), insulin (5 mg/l), transferrin (5 mg/l), streptomycin (100 μg/ml), and penicillin (100 U/ml). After a 3-h attachment period, the culture medium was replaced by the same medium supplemented with dexamethasone (10^{-7} M) and epidermal growth factor (20 ng/ml). Cells were maintained in a humidified atmosphere of 5% CO_2, 95% air at 37°C.

Stable K8-Knockdown and Empty Vector H4-II-E-C3 Cells

Stable K8-knockdown (shK8b) and empty vector (H4ev) H4-II-E-C3 cells have been generated by short hairpin RNA technique as described previously (Galarneau *et al*., 2007). Cells were maintained in DMEM supplemented with 10% FBS and neomycin at 37°C in a humidified atmosphere of 5% CO_2, 95% air.

Cell Attachment and Spreading

Attachment and spreading assays were performed as described previously (Galarneau *et al*., 2007). In some experiments, cells were collected and incubated for 30 min before seeding with dimethyl sulfoxide (vehicle**)** or with 100 nM PMA alone or in combination with 1 μM BIM or Gö.

Cell Migration

Two complementary assays were used to provide evaluations of collective cell migration and single cell locomotion, respectively: collective cell migration assay and single-cell locomotion assay.

Collective Cell Migration Assay. For H4ev and shK8b cells, scratch wounds were created across the cell monolayer with a sterile plastic micropipette tip, and the collective cell migration was assessed by phase-contrast images captured at 10-min intervals over a 20-h period, as described previously (Besson *et al*., 2002; Vomastek *et al*., 2007). WT and K8-null hepatocyte were plated at a density of 1.5×10^5 cells/cm^2 inside 0.22-cm^2 Culture-Insert (Ibidi, Martinsried, Germany). The culture-insert was removed after 24 h of culture, and collective migration was assessed as described above. In some experiments, the monolayer was pre-treated with BIM, Gö, PP2 (25 μM), and/or PMA 30 min before the assay. Cell cultures were observed with a wide-field digital imaging system (TE2000 inverted microscope [Nikon, Tokyo, Japan], HQ CoolSNAP camera [Photometrics, Tucson, AZ], and MetaMorph software [Moleculare Devices, Sunnyvale, CA]) equipped with an environmental chamber. Phase-contrast images were captured at 10-min intervals over a 20-h period, by using a 10×/numerical aperture (NA) 0.5 ph1 dry objective.

Single-Cell Locomotion Assay. A modified version of the procedure described by Chon *et al*. (1997) was used. H4ev and shK8b cells were seeded at a density of 10^4 cells/cm^2 in dishes precoated with fibronectin, and then they were allowed to attach and spread for 2 h, i.e., complete spreading. They were then incubated for 30 min with the fluorescent probe calcein (1 μM), pretreated with BIM or Gö for an extra 30-min period, and then cell locomotion was assessed using fresh medium containing the inhibitor in presence or absence of PMA. Phase-contrast or fluorescence images were captured at 10-min intervals over a 3-h period, by using a 20×/NA 0.5 ph1 dry objective. The cell locomotion was tracked using ImageJ software (National Institutes of Health, Bethesda, MD). The procedure allowed us to assess the relative contribution of PKCα, PKCδ, and PKCε in mediating H4ev versus shK8b cell migration. Accordingly, the locomotion of individual cells was measured following a 48-h transfection with 25 nM control siRNA, PKCα siRNA, PKCδ siRNA, and PKCε siRNA. The transfections were performed with the TransIT-TKO transfection Reagent (MIR2154; Mirus, Madison, WI), according to the manufacturer's instructions; the PKC down-regulation was monitored by Western blotting.

Western Blotting

Total proteins were extracted with preheated (90°C) 2× sample buffer (Gilbert *et al*., 2001). Ten to 20 μg was subjected to SDS-polyacrylamide gel electrophoresis (PAGE) and electrotransferred onto a polyvinylidene difluoride membrane. The blots were incubated with the primary antibody for 16 h at 4°C and then with the appropriate horseradish peroxidase-conjugated secondary antibody for 1 h at room temperature. Signal was revealed with the SuperSignal West Pico kit (Pierce Chemical, Rockford, IL) or Chemiluminescent Peroxidase Substrate (Sigma Sigma-Aldrich Canada).

RACK1 Immunoprecipitation

Cells in suspension were prepared as described above for the spreading assay. For protein extraction, $3{,}5 \times 10^6$ cells were allowed to attach on 15-cm dishes precoated with fibronectin for the indicated time, and the proteins were extracted as described previously (Liao and Omary, 1996) with Empigen BB (Calbiochem, LaJolla, CA). Extracted proteins (300 μg) were precleared with 20 μl of protein G-Sepharose (GE Healthcare, Little Chalfont, Buckinghamshire, United Kingdom) for 1 h at 4°C and then combined to 25 μl of protein G-Sepharose precoated with 1 μg of RACK1 antibody followed by incubation overnight at 4°C with agitation. Beads were recovered by centrifugation for 1 min at 10,000 × *g* at 4°C and washed three times with 500 μl of washing buffer; the supernatant provided the flowthrough fraction. The beads were suspended in 40 μl of SDS sample buffer and submitted to SDS-PAGE and Western blotting.

Subcellular Proteome Extraction

The detergent-based extraction of proteins from the cytosolic (F1), membrane/organelle (F2), nuclear (F3), and cytoskeletal (F4) fractions of H4 cells or hepatocytes was performed with the ProteoExtract subcellular proteome extraction kit (Calbiochem), according to the manufacturer's protocol, as described above; GAPDH (cytosol), superoxide dismutase-2 (mitochondria), histone H3 (nucleus), and lamin/K18 (cytoskeleton) were used as fraction markers (Mathew *et al*., 2008). Of additional note, the surface membrane receptor Fas is present in F2 and F4 (Gilbert *et al*., unpublished data).

Confocal Cell Imaging

β1-Integrin. At 60-min postseeding, the cells were washed twice with phosphate-buffered saline (PBS) and then fixed for 10 min at room temperature with 4% paraformaldehyde in PBS. Next, they were incubated 1 h at room temperature with anti-β1-integrin Alexa 488-tagged antibody (1/100 in PBS).

Vinculin. At 60-min post seeding, the cells were washed twice with PBS, fixed for 10 min at room temperature with 3.7% formaldehyde in PBS, followed by methanol/acetone (3:7) for 5 min at −20°C. They were then incubated overnight at 4°C with anti-human vinculin antibody (1/400 in PBS), followed by 1-h incubation with Alexa Fluor 488 anti-mouse IgG antibody at room temperature.

RACK1, c-Src, PKCα, or PKCδ. Cells were washed twice with PBS, fixed for 10 min at room temperature with 4% paraformaldehyde in PBS, followed by permeabilization with 0.01% Triton X-100 (with 1% bovine serum albumin [BSA] in PBS) at room temperature for 1 h. They were then incubated overnight at 4°C with anti-RACK1 (1/100 in PBS), anti-c-Src (1/20 in PBS), anti-PKCα (1/20 in PBS), or anti-PKCδ (1/100 in PBS), and then for 1 h at room temperature with Texas Red-goat anti-mouse IgM or Alexa-555 anti-mouse IgG, respectively, with anti-β1-integrin Alexa 488-tagged antibody (1/100 in PBS).

Plectin or K8. Cells were washed twice with PBS, fixed for 10 min at room temperature with 3.7% formaldehyde in PBS, followed by methanol/acetone (3:7) for 10 min at −20°C. They were then incubated successively overnight at 4°C with anti-plectin (1/50 in PBS) or with with anti-rat K8 (1/100 in PBS) followed with Alexa Fluor 488 anti-rabbit IgG or with Alexa Fluor 647 anti-mouse IgG antibody, respectively, at room temperature with anti-β1-integrin antibody (1/100 in PBS).

Talin. Cells were washed twice with PBS, fixed for 10 min at room temperature with 3.7% formaldehyde in PBS, followed by methanol/acetone (3:7) for 10 min at −20°C. They were then incubated successively, overnight at 4°C with anti-plectin (1/50 in PBS) or with anti-rat K8 (1/100 in PBS) followed with Alexa Fluor 488 anti-rabbit IgG or with Alexa Fluor 647 anti-mouse IgG antibody at room temperature, respectively, and in combination with anti-β1-integrin antibody (1/100 in PBS).

Caveolin-1. At 48 h postseeding, the cells were washed twice with PBS and fixed for 15 min at room temperature with 4% paraformaldehyde/PBS. Then, samples were rinsed three times in PBS for 5 min and blocked for 60 min in a blocking buffer (5% normal rabbit serum and 0.3% Triton X-100 in PBS). Samples were incubated overnight at 4°C in a humid box with anti-rabbit caveolin antibody diluted 1/200 in antibody dilution buffer (1% BSA and 0.3% Triton X-100 in PBS), followed by a three-time washing in PBS for 5 min and 90-min incubation with Alexa Fluor 488 anti-rabbit IgG antibody at room temperature in the dark.

After immunostaining, samples were rinsed three times in PBS and mounted with a glycine buffer (0.2 M; pH 8.6) 50%/glycerol 50% mounting medium. Images were captured with an FV1000 confocal system (Olympus Canada, Markham, ON, Canada), using the 488, 543 and 633 nm excitation laser lines and a 100×/1.40 NA oil immersion objective. Quantification of protein colocalization after image acquisition was based on the calculation of the Pearson's *r* (Humphries *et al*., 2007). To that end, two captured images were background subtracted, an overlay image was created, a threshold was set to restrict the analysis to an FA region, and the *r* value was calculated by using the Volocity software (Improvision/PerkinElmer, Woodbridge, ON, Canada).

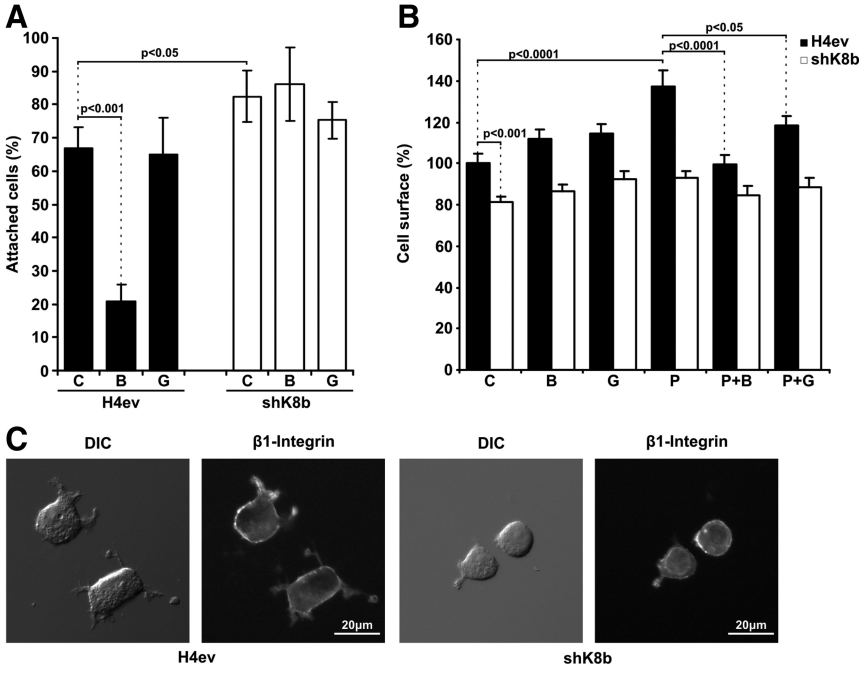

Figure 1. PKC requirement in the K8/K18 modulation of hepatoma cell attachment and spreading. H4ev and shK8b cells were maintained in serum-free media for 24 h before cell dispersion and subsequent seeding in fibronectin-coated dishes. (A) Cell attachment was assayed in absence (C) or presence of BIM (B) or Gö (G). Cells were fixed at 10-min postseeding time, and attached cells were counted in 10 randomly chosen fields per dish. The number of attached cells at 1 h, in absence of inhibitor, was taken as 100%, based on our previous published data (Galarneau *et al*., 2007) (B) Cell spreading was assayed in absence (C) or presence of BIM (B), Gö (G), PMA (P), or in combination with BIM (P+B) or Gö (P+G). Cells were fixed at 60 min postseeding, and the area of at least 36 cells per time point was calculated. The graph shows the mean cell surface (%) values in reference to H4ev cell surface (100%). (C) DIC image of H4ev and shK8b cells fixed at 1 h postseeding and corresponding wide field fluorescence images of Alexa Fluor 488 anti-β1-integrin. The mean values ± SEM of three independent experiments, plus the p values <0.05, are provided.

Fluorescence Recovery after Photobleaching (FRAP)

Cells were transfected using the FuGENE HD Transfection Reagent (Roche Diagnostics, Indianapolis, IN) following the manufacturer's instructions. Cells expressing GFP-FAK or GFP-vinculin were cultured at high density, and scratch wounds were made across the monolayer. FRAP experiments were performed with an FV1000 confocal system (Olympus Canada) equipped with an SIM unit and an environmental chamber, according to a protocol described previously (Goodwin and Kenworthy, 2005). Photobleached regions consisted of a rectangular region (2 μm wide) enclosing a selected FA at the migrating front. Fluorescence within the region was measured at low laser power before bleaching and then photobleached with five iterations at 405 nm by using the SIM unit at 100% laser power. Recovery was monitored at 488 nm at 0.5-s time intervals for 50 s for GFP-FAK, 90 s for GFP-paxillin, and 120 s for GFP-vinculin. In some experiments, cells expressing GFP-FAK were pretreated with 1 μM BIM. Fluorescence during recovery was normalized to the prebleach intensity and for the bleaching occurring during image acquisition, as described previously (Goodwin and Kenworthy, 2005). Relative recovery rates were computed with the Prism (GraphPad Software, San Diego, CA). The half-time for fluorescence recovery toward the asymptote was extracted from the plots after curve fitting of the data to a single exponential association algorithm.

Quantification of FA Dynamics

A modified version of an adhesion dynamics assay (Webb *et al*., 2004) was used to measure FA disassembly rate. In brief, an Ultraview Spinning Disk imaging system (PerkinElmer) was used to perform time-lapse imaging on cells expressing GFP-FAK or GFP-paxillin. The fluorescence of individual FA was measured as function of time with the Volocity software, and the background fluorescent intensity subtracted. No bleaching was observed during the assay. The disassembly dynamics of FAK- and paxillin-containing FAs was reported on a semilogarithmic plot of the fluorescence intensity as function of time. The disassembly rates were computed from the slope of the linear regression on these graphs with the Prism software. Each disassembly rate constant was calculated from measurements performed on 12–15 individual FAs in five cells.

Statistical Analysis

Two groups of data were compared by performing a *t* test statistical analysis using Matlab software (The Mathworks, Natick, MA). A p value <0.05 is considered statistically significant.

RESULTS

PKC Requirement in the Differential Adhesion of H4ev and shK8b Cells

We have shown previously that both K8-null hepatocytes and shK8b cells attach more efficiently but spread more slowly on fibronectin than their counterparts, namely, WT hepatocytes and H4ev cells (Galarneau *et al*., 2007). These α5/β1-integrin-dependent processes occurring at FAs have been reported to depend on PKC-mediated signaling events (Ng *et al*., 1999; Besson *et al*., 2002). As shown in Figure 1A, nontreated shK8b cells attached more efficiently than H4ev cells during the first 10-min period, and a pretreatment with BIM, an inhibitor of both conventional and novel PKCs, led to a threefold reduction in H4ev cell attachment on fibronectin, whereas a pretreatment with Gö, an inhibitor of conventional PKCs only, had no significant effect. However, BIM or Gö did not significantly affect the spreading of H4ev and shK8b cells, respectively (Figure 1B). But upon addition of PMA, an activator of conventional and novel PKCs, we observed a significant increased spreading of H4ev cells, but not of shK8b cells as result of the K8/K18 loss (Figure 1B). Notably, this H4ev cell PMA spreading induction was inhibited by a pretreatment with BIM (Figure 1B), whereas Gö was unable to provide a complete reduction in spreading. Moreover, in line with our previous fluorescence-activated cell sorting data (Galarneau *et al*., 2007), β1 integrin immunostaining on nonpermeabilized cells revealed a comparable integrin exposure at the surface of H4ev versus shK8b cells (Figure 1C), meaning that the reduction in shK8b cell spreading was not due a difference in integrin recruitment at FAs.

The tandem adaptor talin/vinculin, known to link integrins to actin, has been shown to orchestrate the formation and distribution of FAs (Geiger *et al*., 2001; Humphries *et al*., 2007). Using vinculin as a FA marker, we have reported before that the K8/K18 loss perturbed the FA status in spreading hepatocytes (Galarneau *et al*., 2007), and our data in spreading hepatoma cells provided similar FA perturbations (Supplemental Figure S1). We thus examined to which extent this K8/K18 modulation of the FA distribution occurs through a PKC mediation. As shown in Supplemental Figure S1, a PKC stimulation with PMA had minimal effect on the FA size but resulted to a FA alignment at the margin of both H4ev and shK8b cells, which was reversed by BIM but not Gö. Together, these results indicate that the K8/K18

modulation of hepatoma cell spreading does not occur through direct structural changes at FAs, but probably through a novel PKC mediation of integrin signalization and related FA dynamics.

PKC-mediated Differential Migration of H4ev versus shK8b Cells

In addition to their role in cell spreading, there is ample evidence for a key involvement of PKCs in the regulation of integrin-dependent cell migration (Buensuceso *et al*., 2001; Besson *et al*., 2002; Vomastek *et al*., 2007). We thus sought to assess to which extent the K8/K18 loss affects hepatoma cell migration and whether it occurs through a novel PKC mediation. We first examined cells migrating collectively, by using the scratch-wound assay. As shown in Figure 2, A and B, compared with H4ev cells, shK8b cells exhibited a slower migration during a 20-h period, implying that K8/K18 contribute to the induced migration of hepatoma cells. Moreover, in light of the above-mentioned data on cell spreading, we assessed the migration of H4ev versus shK8b cells with or without PMA, in the presence or absence of BIM or Gö. As shown in Figure 2B, a pretreatment with BIM alone resulted in a significant reduction in H4ev but not shK8b cell migration. In parallel, a PMA pretreatment amplified the differential migration response of H4ev versus shK8b cells, which was significantly inhibited by BIM but not by Gö (Figure 2B). These data can be visualized in the attached videos (Fig 2B_H4ev.mov, Fig 2B_shK8b.mov, Fig 2B_H4evPMA.mov, and Fig 2B_shK8bPMA.mov). It is worth noticing that no cell death occurred during the spreading process. By combining these results with the cell attachment/spreading data (Figure 1), we concluded that a novel PKC(s) mediates the K8/K18 modulation of hepatoma cell adhesion and migration.

Of particular note, because c-Src constitutes an intermediary regulator of cell migration (Wu *et al*., 2008), we assessed its requirement in PKC-mediated migration of H4ev versus shK8b cells. As shown in Supplemental Figure S2, a pretreatment with PP2, a Src family inhibitor, led to a migration reduction to identical levels for both cell types. In addition a PP2 pretreatment in presence of PMA in this case yielded a return at control levels, i.e., not at the level of PP2 alone. Our interpretation is that the differential PKC-mediated migration is in part c-Src independent.

PKCδ as Preferential Mediator of the K8/K18 Modulation of H4 Cell Adhesion/Migration

Although BIM and Gö are quite reliable as tools for evaluating the contribution of conventional versus novel PKCs in cell adhesion and migration, the available chemical inhibitors that have been proposed to distinguish PKCs within each subfamily are not necessarily reliable. Moreover, the wound-scratch assay implies a 20-h cell locomotion of not only cells at the migration front but also those behind in the monolayer, which may respond differently to PKC inhibition. So, to address these technical limitations, we used siRNA-mediated knockdown procedure to assess the relative capacity of PKCα, PKCδ, and PKCε in mediating H4ev versus shK8b cell migration, by using a single-cell locomotion assay at the 3-h postseeding period, at which time the cells are fully spread. As expected, under control conditions H4ev cells and shK8b cells exhibited a similar locomotion in term of travel distance, i.e., between the starting and final points (Figure 3, A, B, and E). Moreover, the addition of BIM slightly increased the H4ev cell travel distance, whereas Gö exerted a low stimulation on shK8b cell travel distance (Figure 3E). A PMA pretreatment increased preferentially the

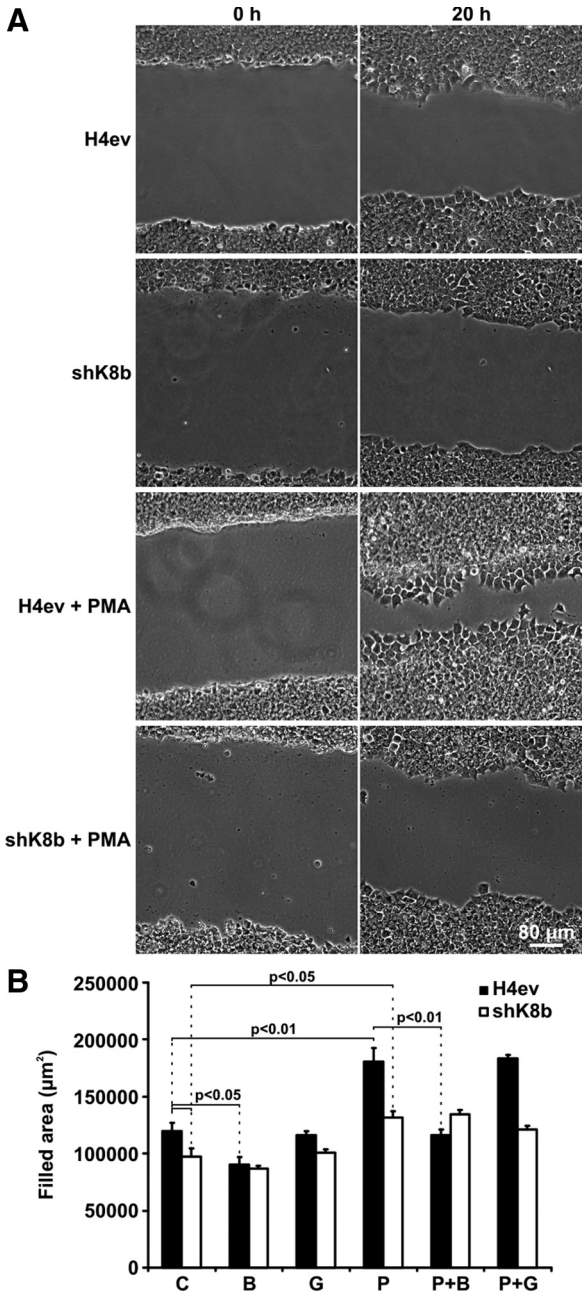

Figure 2. PKC requirement in the K8/K18 modulation of collective hepatoma cell migration. Scratch wounds were made in confluent cultures of H4ev and shK8b cells. (A) Phase-contrast images were taken immediately after scratching (0 h) and at 20 h postscratching. Cells were pretreated with vehicle (control) or PMA. (B) Quantification of the wound closure at 20 h postscratching of cells pretreated with vehicle (C), BIM (B), Gö (G), PMA (P), PMA + BIM (P+B), or PMA + Gö (P+G). The mean values ± SEM of three independent experiments, plus the p values <0.05, are provided.

travel distance of H4ev cells over shK8b cells (Figure 3, C–E). However, for both cell types, the PMA-induced distance was inhibited by BIM, but not Gö (Figure 3E). As shown in Figure 3F, efficient knockdowns of PKCα, PKCδ, and PKCε were obtained at 48 h posttransfection. The PKCα knockdown had no effect on the migration of either H4ev or shK8b cells (Figure 3G). The PKCδ knockdown led to a massive reduction in the PMA-stimulated migration of H4ev cells,

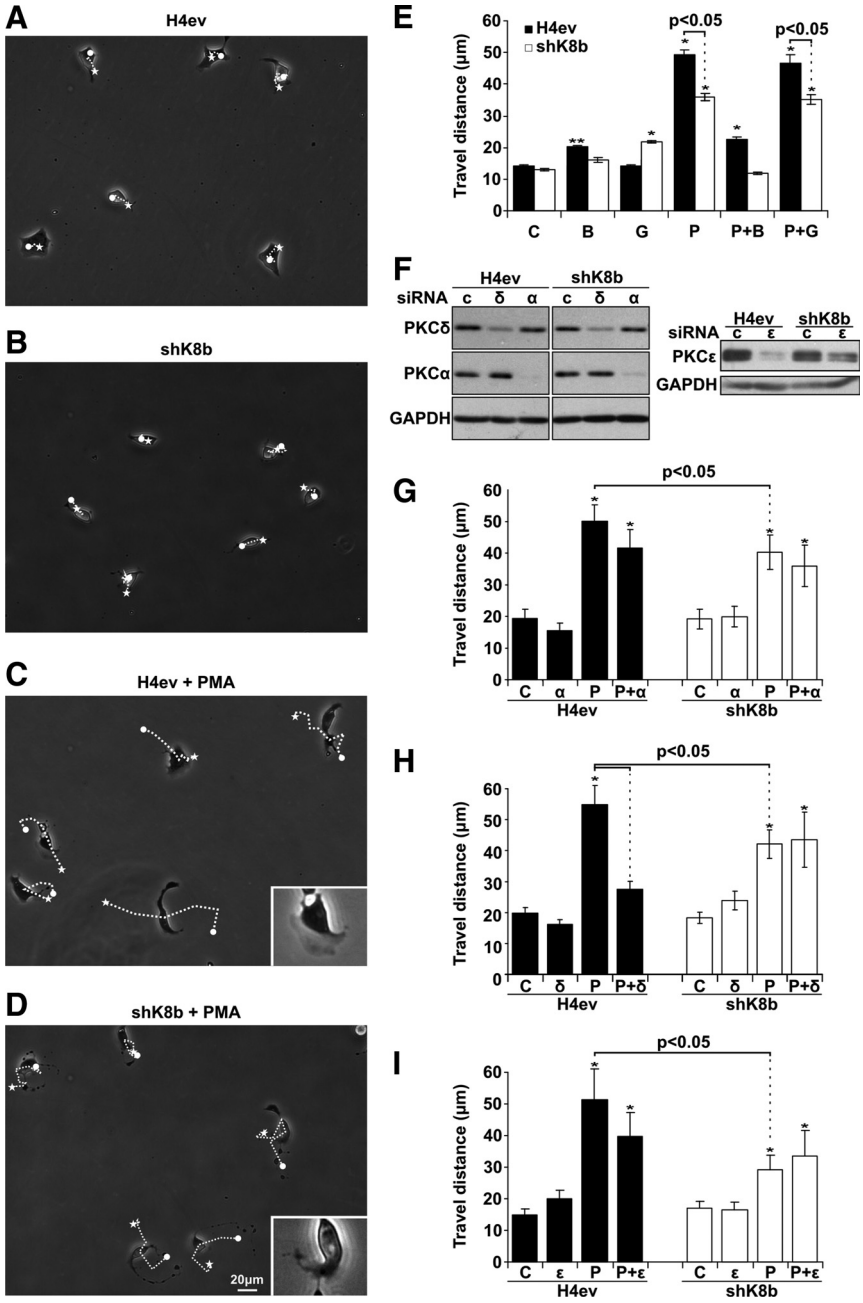

Figure 3. PKC requirement in the K8/K18 modulation of single-hepatoma cell locomotion. (A–D) Phase-contrast images of the cell locomotion were taken during 3 h after treatment with vehicle (A and B, respectively) and PMA (C and D). The dotted lines correspond to the locomotion paths during the 3-h period. Insets in C and D show migrating cells with lamellipodia. (E) Histograms showing the mean travel distance ± SEM (linear gap between white dot and star in A–D) calculated for 60 cells per experiment. Cells were treated with vehicle (Control, C), BIM (B), Gö (G), PMA (P), PMA + BIM (P+B), or PMA + Gö (P+G). (F) Western blotting on total cell extracts prepared from H4ev and shK8b showing the diminution in protein content of PKCδ (δ), PKCα (α), or PKCε (ε) at 48 h posttransfection of the respective siRNA. C, control siRNA. (G) Histogram showing the mean travel distance of H4ev and shK8b cells transfected with control siRNA (C) or with PKCα siRNA (α) and further treated with PMA (P). (H) Histograms showing the mean travel distance of H4ev and shK8b cells transfected with control siRNA (C) or with PKCδ siRNA (δ) and further treated with PMA (P). (I) Histogram showing the mean travel distance of H4ev and shK8b cells transfected with control siRNA (C) or with PKCε siRNA (ε) and further treated with PMA (P). The p values <0.05 are provided; *$p < 0.01$ relative to control.

but not of shK8b cells (Figure 3H). In comparison, the PKCε knockdown did not lead to a significant reduction in the PMA-stimulated migration of H4ev cells, but not of shK8b cells (Figure 3I). Overall, the data indicated that although PKCδ was required for the migration of H4ev cells, the K8/K18 loss rendered the migration of shK8b cells PKCδ independent.

PKC Mediation of FAK Activation in Adhering H4ev and shK8b Cells

PKCδ activation is a rather complex process that involves a series of sequential phosphorylations, including a PDK1 or PKCε-dependent activation-loop phosphorylation on Thr-505, which in turn plays a distinctive role in generating a fully competent form of activated PKCδ (Rybin *et al.*, 2007). So, using Thr-505 phosphorylation as an activation event, we assessed the PKCδ activation kinetics in adhering H4ev and shK8b cells. Notably, a relatively high PKCδ activity was detected in both cell suspensions followed by a 60–80% drop during the first 10- to 20-min attachment, and a subsequent small increase activity that reached a maximum at 60 min in H4ev cells and a gradual slight increase over the 120-min spreading period in shK8b cells (Figure 4, A and B). However, a PMA pretreatment led to higher PKCδ activation with a maximum at 60 min in both cell types, with no significant increase ($p > 0.05$) on the PKCδ phosphorylation in shK8b cells (Figure 4, A and C). As expected, the presence of BIM brought the differential PKCδ phosphorylation levels back to those observed in the non-PMA–treated cells.

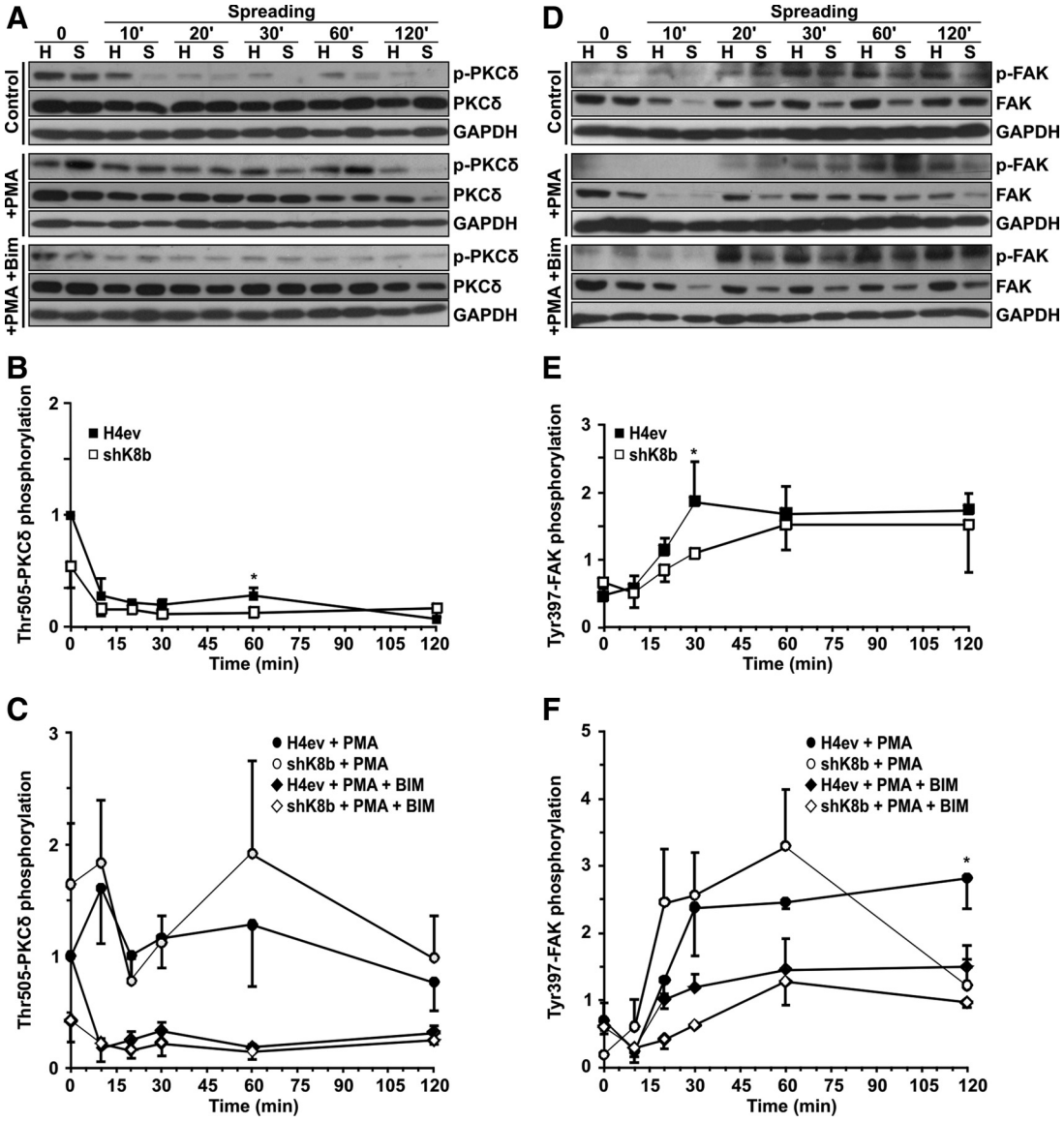

Figure 4. PKCδ and FAK activations in spreading H4ev and shK8b cells. Western blotting on total protein extracts from H4ev (H) and shK8b (S) cells at indicated postseeding times on fibronectin. (A) PKCδ phosphorylation on Thr-505 and (D) FAK phosphorylation on Tyr-397 (FAK; p-FAK) in presence of vehicle (control), PMA, or PMA + BIM. H4ev and shK8b densitometric quantifications of PKCδ (B and C) and FAK (E and F) phosphorylation levels normalized over the total respective PKCδ and FAK levels at 2 h postspreading, in absence (B and E) or presence of PMA and PMA + BIM (C and F). GAPDH was used as loading control. The mean densitometric values ± SEM of three independent experiments are provided. *$p < 0.05$ for H4ev versus shK8b, and H4ev + PMA versus shK8b + PMA conditions.

FAK activation, as monitored by its autophosphorylation at Tyr-397, reflects a primary signaling step triggered by β1-integrin engagement on fibronectin (Hamadi *et al*., 2005). We thus used this signaling endpoint in an attempt to position the K8/K18 modulation of the PKC-mediated signaling of the hepatoma cell spreading. As shown in Figure 4, D and E, the integrin engagement induced an FAK activation that started at 20 min postseeding and peaked at 30 min in H4ev cells and at 60 min in shK8b cells. Of note, the FAK content also was reduced in shK8b cells (Figure 4D), which is in line with our previous report revealing a reduction in plectin and β1-integrin expression at shk8b cell surface, along with a 20% reduction in total protein (Galarneau *et al*., 2007). In addition, previous work on cultured muscle cells has indicated that PKC is involved in a positive feedback loop of the integrin/FAK-dependent signaling, a cycle that seems to be essential for cell spreading (Disatnik and Rando, 1999). Notably, in line with the above-mentioned PKCδ activation kinetics, a PMA pretreatment led to a stronger but transient FAK activation with the maximum remaining at 60 min in shK8b cells, with little additional effect on the FAK response in H4ev cells (Figure 4, D and F). Intriguingly, as observed with the PKCδ kinetics, the relative increase in FAK Tyr-397 level was higher in shK8b cells than in H4ev cells, in spite of their slower spreading (Figure 1B), suggesting a dysfunctional PKCδ/FAK signaling as result of the K8/K18 loss. Nevertheless, the presence of BIM led to a return in the differential FAK phosphorylation observed in the non-PMA–treated H4ev versus shK8b cells. Overall, the data confirm that a signaling link exists between PKCδ and FAK in H4 hepatoma cells and that a K8/K18 loss perturbs the PKC contribution to the integrin/FAK positive feedback loop.

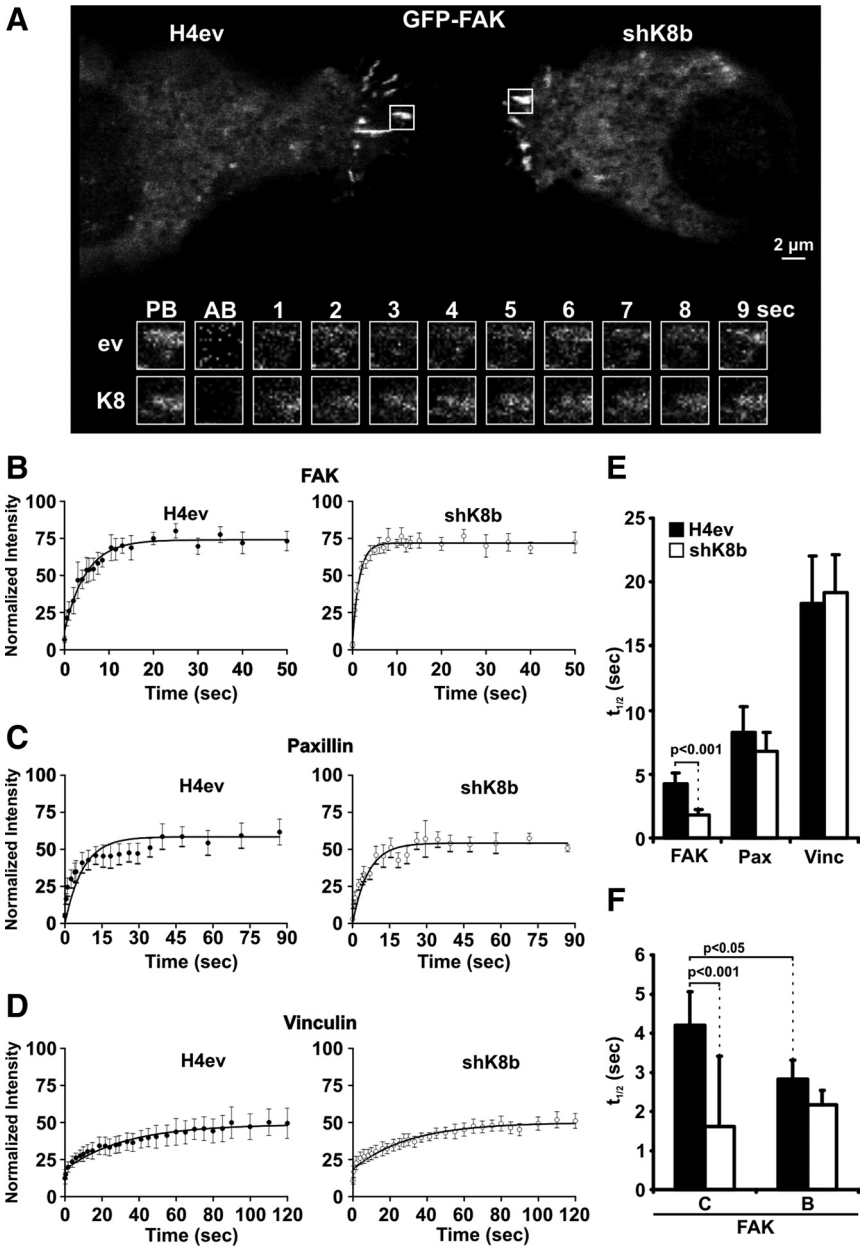

Figure 5. Residency of FAK, paxillin, and vinculin at FAs in spreading H4ev and shK8b cells. (A) Confocal live cell images of H4ev (left) and shK8b (right) cells expressing GFP-FAK were taken before photobleaching the regions of interest (ROIs) (white squares) containing FAs. Time-lapse sequence (below, in seconds) of the selected ROIs show recovery after photobleaching for H4ev cells (ev, top row) and shK8b cells (K8, bottom row). PB, prebleach; AB, immediately after photobleaching. Kinetics of recovery of GFP-FAK (B), GFP-paxillin (C), and GFP-vinculin (D) after photobleaching of FAs from H4ev (top) or shK8b (below) cells is illustrated. The measured fluorescence intensity in eight independent ROIs per cell type was normalized and the mean values ± SEM are shown. The histogram in E depicts the recovery half-time ± SEM obtained from FRAP analyses of GFP-FAK (FAK), GFP-paxillin (Pax), and GFP-vinculin (Vinc) in H4ev and shK8b cells. The histogram in (E) depicts the recovery half-time ± SEM obtained from FRAP analyses of GFP-FAK in cells pretreated with vehicle (C) or BIM (B).

FAK Residency at FAs in Migrating H4ev and shK8b Cells

In light of the above-mentioned data showing that the K8/K18 loss perturbed FAK activation and protein levels during H4 cell spreading, and considering that cell spreading constitutes a primary event associated with remodeling and reorganization of FAs upon cell migration (Hamadi *et al.*, 2005), we extended our FAK analysis to assess its residency at FAs during H4ev versus shK8b cell migration. Remarkably, measurements of the recovery half-time after photobleaching (FRAP analysis) of GFP-FAK yielded an average value of 4.3 s in H4ev cells, compared with 1.2 s in shK8b cells, implying that the reduced migration of these K8/K18-lacking hepatic epithelial cells was associated with a greater FAK turnover (Figure 5, A, B, and E). Paxillin, an important partner of FAK signaling, can be recruited to FAs independently of FAK by vinculin (Humphries *et al.*, 2007). We thus assessed the dynamics of this protein to determine the specificity of the K8/K18 action on FAK residency. As shown in Figure 5, D and E, FRAP measurements on paxillin revealed a minimal but not significant K8/K18-dependent reduction in the paxillin recovery half-life, with values of 8.2 and 6.8 s at FAs of H4ev and shK8b cells, respectively. Moreover, in support of the primary role of vinculin in FA formation (Humphries *et al.*, 2007), the present FRAP measurements of vinculin residency yielded much longer, and again with no K8/K18-dependent effect on the recovery half-times, respective values of 18.3 and 19.2, at H4ev and shK8b cell FAs (Figure 5, C and E). Moreover, parallel measurements of FA turnover during a 20-min period, by using either GFP-FAK or -paxillin and time-lapse confocal imaging, revealed a one-third reduction in the disassembly rate in shK8b cells (Supplemental Figure S3), implying a perturbation in the FA dynamics as result of the K8/K18 loss. Finally, in light of the above-mentioned data on the K8/K18 modulation of FAK residency and the previous data on cell attachment and FAK activation (Figures 1A and 4), we extended our PKC inhibi-

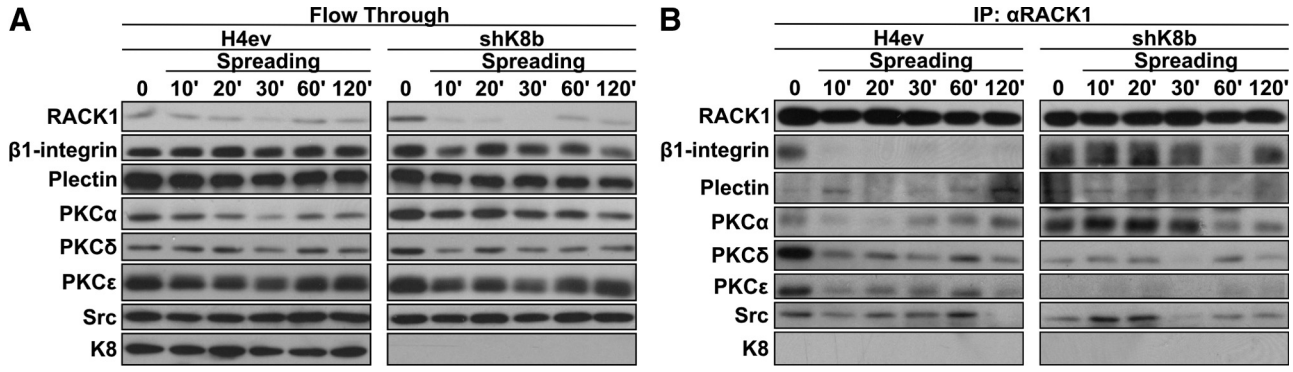

Figure 6. Complex formation between RACK1, β1-integrin, plectin, PKCs, and Src in spreading H4ev and shk8b cells. Cells were maintained in serum-free media for 24 h before their seeding on fibronectin, proteins were solubilized with Empigen, RACK1 was immunoprecipitated, and the flowthrough was kept. (A) Western blotting with antibodies against β1-integrin, plectin, PKCα, PKCδ, PKCε, Src, and K8 in the flow through from the RACK1 immunoprecipitates at the indicated postseeding times. (B) Western blotting with antibodies against the corresponding proteins, after RACK1 immunoprecipitation (IP: αRACK1).

tion analysis to the FRAP recovery half-life measurement. Interestingly, the use of BIM reduced FAK residency in FAs to 2.8 s in H4ev cells, whereas it was maintained ≈2.0 s in shK8b cells (Figure 5F). Thus, the K8/K18 loss impairs the PKC-mediated FAK recruitment/stabilization at FAs, consistent with impaired shK8b cell spreading. Together, these data confirm the preponderance of PKC-FAK signaling over vinculin/actin coupling as intermediary in the K8/K18-dependent modulation of integrin-mediated spreading and migration in hepatoma cells.

RACK1/β1-Integrin/Plectin/PKC/c-Src Interplay in Spreading H4ev and shK8b Cells

RACK1 is known to provide a link between PKC and β1-integrin in cultured glioma cells (Besson *et al*., 2002) and to interact with plectin during cell adhesion (Osmanagic-Myers and Wiche, 2004) and, as mentioned above, plectin binds to different types of IF proteins, including K8/K18 (Reznicek *et al*., 2004). We thus examined the time/composition differences in RACK1, β1-integrin, plectin, PKCα, PKCδ, and PKCε complex formation in H4ev versus shK8b cells. To that end, proteins from whole H4ev and shK8b cell lysates taken at different postseeding time points were solubilized with Empigen, RACK1 was immunoprecipitated and the flowthrough kept, and then the binding partners were identified by Western blotting. Of note, the blotting data from the flowthrough indicated that all the proteins were solubilized at comparable levels, respectively, at all time points (Figure 6A). As shown in Figure 6B, we confirmed that RACK1 was present in the isolated complexes from both cell populations at all time points. Intriguingly, although β1-integrin was present only at time 0 in H4ev cells, it remained present at the subsequent time points in shK8b cells, with a maximum occurring at 20 min postseeding. Plectin was found at a low level in the immunoprecipitation (IP) complex at all time points in both cell populations. PKCα largely matched the time-dependent content of β1 integrin in the IP complex. PKCδ and PKCε were both predominant at time 0 in H4ev cells, but PKCε was essentially excluded of the complex at any postseeding periods in shK8b cells. Moreover, in line with a previous report showing its capacity to bind RACK1 (Mamidipudi *et al*., 2007), c-Src was present in the complex during the first 60 min postseeding in H4ev cells, whereas it peaked at 10–20 min in shK8b cells. However, despite the use of an Empigen-based procedure, which has been shown to solubilize large amounts of keratins (Liao and Omary, 1996), essentially no K8 was coimmunoprecipitated with this complex. However, the use of the same immunoprecipitation protocol with a radioimmunoprecipitation assay buffer demonstrated the presence of K8/K18 in the RACK1-containing complex (data not shown), indicating that K8/K18 are complex partners. Still, it remains that the immunoprecipitation was performed on detergent-soluble protein preparations from whole cell lysates. So, we used a confocal imaging-based procedure to verify the extent to which the immunocomplex partners were actually detectable at FAs. To that end, we used β1-integrin and talin as FA makers and first confirmed that a coimmunolocalization of talin and β1-integrin indeed occurred at FAs in both H4ev and shK8b cells (Figure 7A). Then, we compared the localization of RACK1, PKCδ, PKCα, c-Src, plectin, and K8 with that of β1-integrin at FAs. Quantification of colocalization in image overlays was performed based on the calculation of the Pearson's *r*. Using talin as a reference FA protein that directly binds β1-integrin and considering 1 as a perfect correlation, the 0.6 values for PKCδ, c-Src, plectin, and K8 reflected very good colocalizations at FAs (Figure 7B). Even though the 0.45 coefficient value for RACK1/β1-integrin indicated less colocalization, β1-integrin was immunoprecipitated with RAKC1, meaning that although RACK1 localized at FAs, a much larger fraction remained in the cytoplasm. In the same way, a localization of the other complex partners at FAs did not exclude their presence in the intracellular compartments. On the overall, the main findings are that a RACK1–plectin–PKC–c-Src interplay occurs in H4ev cells and that a K8/K18 loss in shK8b cells results to alteration of the complex assembly.

K8/K18 Modulation of PKC-mediated Integrin-dependent Adhesion in Nonmigrating Hepatocytes

We have reported before that, as in the case of hepatoma cells, K8-null hepatocytes attach more efficiently but spread more slowly on fibronectin than WT hepatocytes (Galarneau *et al*., 2007). On these grounds, we have assessed the extent to which the K8/K18 modulation was occurring through a PKC mediation. As shown in Figure 8A, we first confirmed that nontreated K8-null hepatocytes attached more efficiently than WT hepatocytes during the first 30-min period, and then we found that a pretreatment with BIM or Gö led to no significant reduction in hepatocyte attachment. Moreover, PMA yielded a 1.9- and 1.5-fold enhancement in WT and K8-null hepatocyte spreading, respectively (Figure 8B),

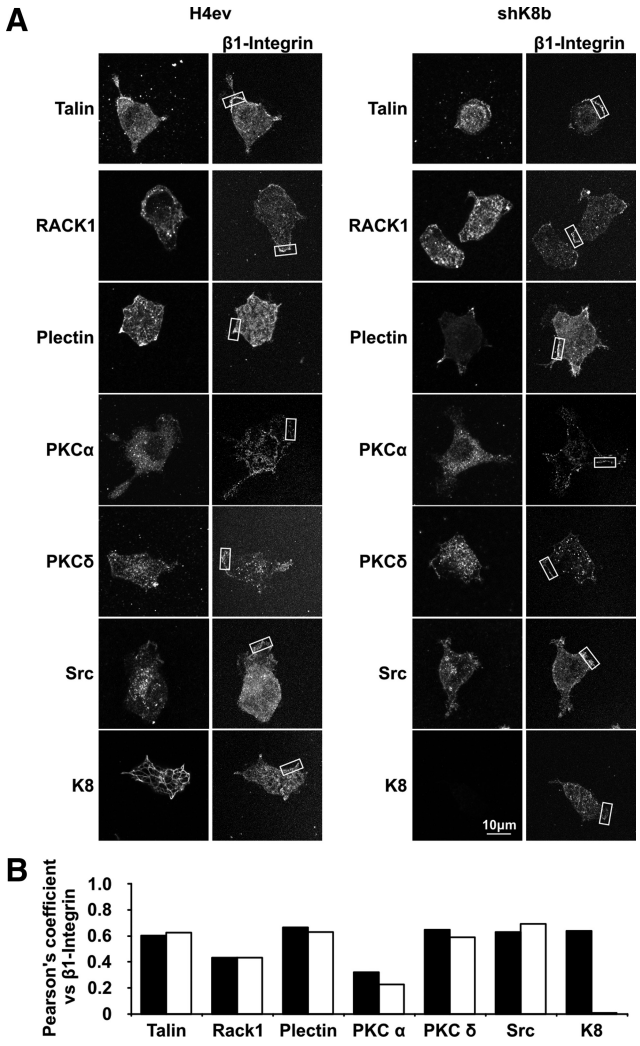

Figure 7. Colocalization of β1-integrin with talin, RACK1, plectin, PKCs, Src, and K8 in spreading H4ev and shk8b cells. (A) Cell were allowed to spread for 1 h and then fixed and colabeled with β1-integrin antibody and the corresponding antibody for the second protein. Images were captured with a FV1000 confocal system. (B) The Pearson's colocalization *r* of each protein versus β1-integrin was computed for a region rich in β1-integrin (boxed area in A).

and notably this PMA spreading induction was readily inhibited by a pretreatment with BIM or Gö, suggesting a predominant PKCα involvement (Figure 8B). As expected, both WT and K8-null hepatocytes constitute nonmigrating simple differentiated epithelial cells (Figure 8, C and D). Hepatocyte motility can be visualized in the attached video (Fig 8C_WT.mov, Fig 8C_K8n.mov, Fig 8C_WTPMA.mov, and Fig 8C_K8nPMA.mov). Still, in line with the data we have reported previously (Galarneau *et al*., 2007), the kinetics of FAK phosphorylation matched with the reduced spreading of K8-null hepatocytes (Figure 8E). Little variation was detected in FAK content in either WT or K8-null hepatocytes. However, unlike with hepatoma cells, a PMA pretreatment led to a difference in FAK phosphorylation only at 60 min between WT and K8-null hepatocytes. The presence of BIM led to a return in the differential FAK phosphorylation observed in the non-PMA–treated hepatocytes.

RACK1, β1-Integrin, Plectin, PKCs, c-Src, and K8 Distributions in Subcellular Fractions

Because the IP results indicate that the nature of the detergent can affect the cohesive formation of the protein complex and because the fluorescence images of the proteins localizing at FA cannot exclude their presence in the intracellular space in H4ev and shK8b cells (Figures 5–7), we used the subcellular proteome extraction assay we had described previously (Mathew *et al*., 2008) to document the relative distributions RACK1, β1-integrin, plectin, PKCs, c-Src and K8, respectively, among the cytosolic (F1), membrane/organelle (F2), nuclear (F3), and cytoskeletal (F4) fractions. Our initial attempts to perform the fractionation on adhering cells turned out to be nonfeasible, so we decided to use H4 cell suspensions and monolayers, the two "initial" conditions for cell adhesion and scratch-induced migration, respectively (Figure 9A). The content of each protein also was assessed in whole cell extracts. For example, in line with our previous data on adhering H4ev and shK8b cells (Galarneau *et al*., 2007), we found that the content of plectin was lower in shK8b than in H4ev cells under both the suspension and monolayer conditions (Figure 9A). Although a little difference in total β1-integrin levels was found in H4ev versus shK8b cells under the suspension condition, its total level was slightly higher in shK8b cells under the monolayer condition. Nevertheless, under the suspension condition, we uncovered a predominant restriction of RACK1 in F1 in H4ev and shK8b cells, a lower β1-integrin level in F2 in shK8b versus H4ev cells, and a large portion of plectin in F2 in H4ev cells compared with F1 and F2 in shK8b cells. In addition, we found a larger PKCδ proportion in F2 in H4ev cells and comparable c-Src in F1 and F2 in both H4ev and shK8b cells. Under the monolayer condition, RACK1 was distributed in F1 and F2, whereas β1-integrin was essentially restricted to F2 in both H4ev and shK8b cells, with a higher level in shK8b cells. Plectin was predominantly found in F4, the most insoluble fraction containing K8 as well. Although PKCα was largely found in F1, the cytosolic fraction, PKCδ and PKCε were distributed in different proportions between F1 and F2 in both H4ev and shK8b cells. Finally, c-Src was distributed among F2, F3, and F4 in a comparable manner between the two cell monolayers. So, we consider that the differential intracellular distributions we observe here for RACK1, β1-integrin, plectin, PKC, and c-Src probably apply to adhering and migrating H4ev and shK8b cells. In this context, we extended our proteome analysis to adhering but nonmigrating hepatocytes (Figure 9B). Of note, the content of β1-integrin, was lower in K8-null than in WT hepatocytes under both the suspension and monolayer conditions. In the same way, as reported before for adhering hepatocytes (Galarneau *et al*., 2007), the K8/K18 loss led to a lower total plectin content under either the suspension or monolayer condition. Under the suspension condition, the main proteome finding was a restriction of RACK1 to F1 and β1-integrin to F4 in both WT and K8-null hepatocytes. Under the monolayer condition, RACK1 was essentially found in F2 and F3 in both WT and K8-null hepatocytes. Moreover, the presence of β1-integrin in F2 and PKCε in F1/F2 was more pronounced in K8-null hepatocytes, whereas PKCα and PKCδ were largely restricted to F1, and c-Src was found at comparable levels in all fractions. Still, it seems that the observed disparity in the ability of hepatocytes versus hepatoma cells to migrate cannot be explained by differences in the subcellular distributions of these integrin-dependent signaling molecules.

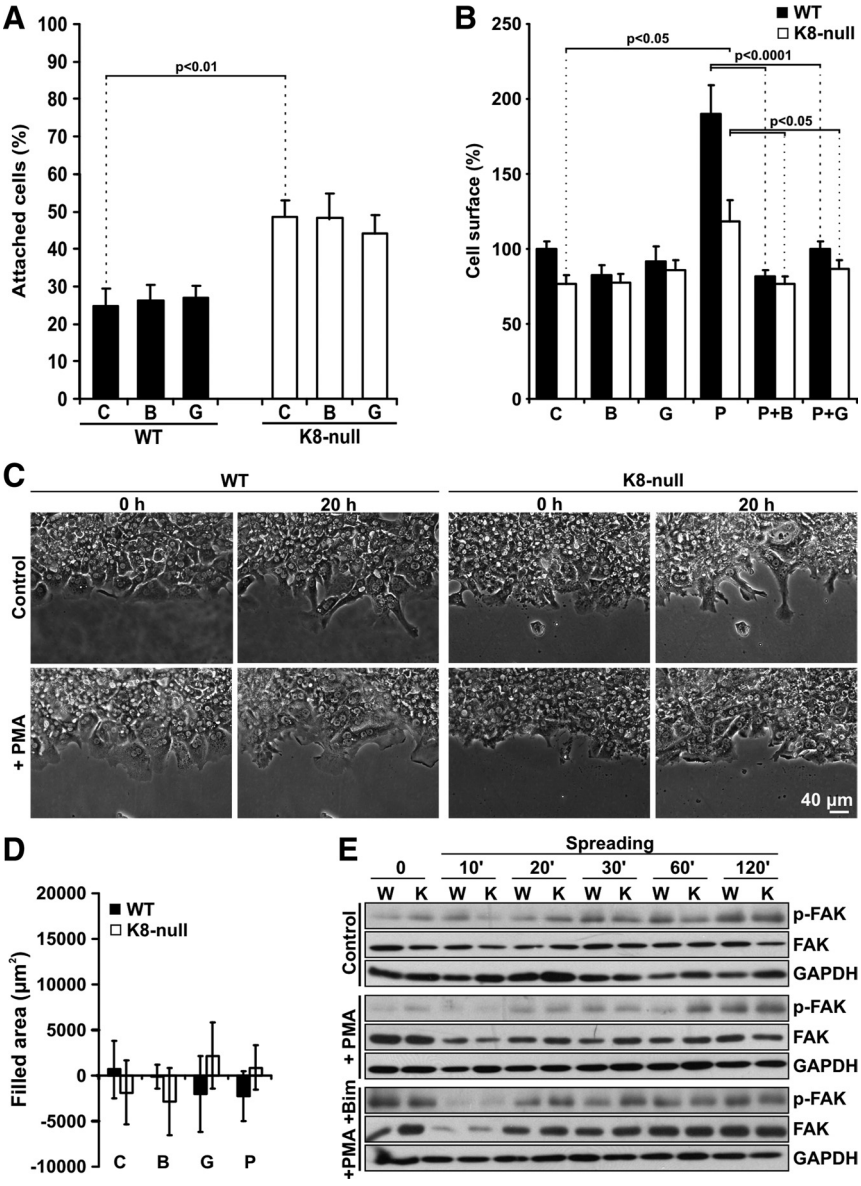

Figure 8. (A) PKC requirement in the K8/K18 modulation of WT and K8-null hepatocyte attachment. The attachment assay was performed in absence (C) or presence of BIM (B) or Gö (G). The cells were fixed at 30 min postseeding, and attached cells were counted in 10 randomly chosen fields per dish. The number of attached cells at 3 h, in absence of inhibitor, was taken as 100%. The mean values ± SEM of two independent experiments are indicated. (B) PKC requirement in the K8/K18 modulation of hepatocyte spreading. WT and K8-null hepatocytes were seeded in absence (C) or presence of BIM (B), Gö (G), PMA (P) or with PMA + BIM (P+B) or PMA + Gö (P+G) and allowed to spread. Images from fixed cells were captured at 60 min postseeding, and the area of 30 cells per time point was calculated. The graph shows the mean cell surface (%) values ± SEM, in reference to WT cell surface (100%). (C) Scratch wound assay on WT and K8-null hepatocyte monolayers, revealing the absence of hepatocyte collective cell migration. Phase contrast images were taken immediately after scratching (0 h) and at 20 h postscratching. Cells were pretreated with vehicle (Control) or PMA. (D) Hepatocyte migration was quantified during the 20-h period, after pretreatment with vehicle (C), BIM (B), Gö (G), or PMA (P). (E) Western blotting on total protein extracts from WT (W) and K8-null (K) hepatocytes at the indicated postseeding times, showing the kinetics of FAK phosphorylation on Tyr-397 (p-FAK) in absence (Control) or presence of PMA or PMA + BIM. GAPDH was used as loading control.

Although a detailed investigation of alternative candidates susceptible of being responsible for the nonmigrating feature of cultured hepatocytes is beyond the scope of the present work, our subcellular distribution analyses of ILK revealed a predominant restriction in F2 in hepatoma cells compared with a relatively even repartition among F2 and F4 in hepatocytes (Supplemental Figure S4A). Notably, parallel analyses yielded subcellular repartitions of cav-1 that matched those of ILK, except for its more obvious presence in the F1 of hepatoma cells. Even more relevant, concomitant confocal immunofluorescence imaging analyses indicated that the preferential restriction of cav-1 in F1/F2 reflected a massive cytoplasmic vesicular localization in hepatoma cells (Supplemental Figure S4B), whereas its F2/F4 repartition in hepatocytes matched with a cytoplasm versus surface membrane distribution (Supplemental Figure S4C). How these results are related to the close link between ILK and cell motility (Gagné *et al*., 2010), and the cav-1/integrin interplay in migrating epithelial cells (Vassilieva *et al*., 2008), deserves future detailed investigation.

DISCUSSION

Much of our knowledge on the signaling-related functions of K8/K18 IFs has come from work examining the link between their phosphorylation at specific Ser sites by various kinases and their rearrangement/solubility under different cellular conditions (Omary *et al*., 2006), including the PKC-mediated reorganization of K8/K18 IFs in alveolar epithelial cells exposed to a shear stress (Ridge *et al*., 2005; Sivaramakrishnan *et al*., 2009). Here, we provide the first direct evidence for the involvement of novel PKCδ as mediator of the K8/K18 modulation of hepatoma cell adhesion and migration, namely, through integrin/FAK-dependent signalization. The relevant components of the integrin-signaling pathways in H4ev versus shK8b cells, in relation to the RACK1/β1-integrin/plectin/PKC/c-Src complex assembled at FAs are depicted in Table 1 and schematically represented in Figure 10A. The K8/K18 loss in shK8b cells modulates the PKC-dependent integrin/FAK feedback loop that normally occurs in H4ev cells (Figure 10B), due to

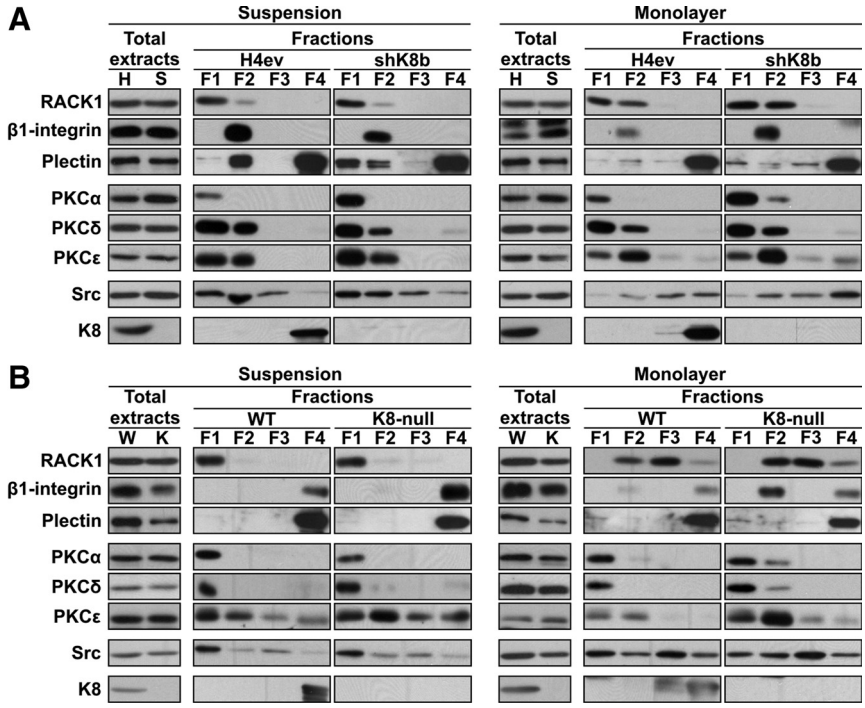

Figure 9. Intracellular distributions of RACK1, β1-integrin, plectin, PKCs, Src, and K8 in hepatoma cells and hepatocytes. Suspensions or monolayers of H4ev (H) and shK8b (S) cells (A) or WT (W) and K8-null hepatocytes (K) (B) separated into fractions enriched in cytosolic (F1), membrane/organelle (F2), nuclear (F3), and cytoskeletal (F4) proteins were analyzed by Western blotting for changes in the relative distributions of the individual proteins. The relative contents the same proteins in the total protein extracts also were determined.

perturbations in the subcellular distribution and interplay of RACK1, integrin, plectin, and other partners (Figure 10C), Notably, although a similar K8/K18-PKC-FAK interplay occurs during the spreading of hepatocytes, these integrin-dependent signaling events are not transduced into migration for either WT or K8-null hepatocytes (Table 1).

Table 1. Relevant components of the integrin-signaling pathways in liver epithelial cells

	Hepatomas		Primary cells	
Observation	H4ev	shK8b	WT	K8-null
Cell attachment	+	+++	+	+++
PKC requirement	Yes	No	No	No
Cell Spreading	+++	+	+++	+
PMA stimulation	High	None	High	Low
PKC requirement	Yes	No	Yes	Yes
Integrin recruitment	++	++	++++	+++++
FA size	++	++	++	++
PMA stimulation	Yes	Yes	N/A	N/A
FAK activation	++++	+++	+++	++
PMA stimulation	+++++[a]	++++++[a]	+++[a]	+++[a]
PKC requirement	Yes	Yes	Yes	Yes
Collective migration	+++	++	−	−
PMA stimulation	+++++	+++	−	−
PKC requirement	Yes	No	N/A	
Src requirement	Yes	Yes		
Single cell locomotion	+	+		
PMA stimulation	+++	++		
PKC requirement	Yes	Yes		
FA protein residency				
FAK	++	+		
PAX	+++	+++		
Vinculin	++++++	++++++		
BIM effect on FAK	+	+		

N/A, not applicable and/or available.

[a] Delayed activation.

Binding of integrins to their ECM ligands activates intracellular signaling cascades, so-called "outside-in signaling," that differ depending on the specific integrin/ligand interaction and the cell type (Disatnik and Rando, 1999). One of the early events initiated by the engagement of integrins is their clustering at FAs associated with the subsequent induction of FAK autophosphorylation at Tyr-397, which in turn is considered as a critical step for the downstream signaling that promotes cell spreading (Hamadi *et al*., 2005; Meng *et al*., 2009). Conversely, cell attachment and spreading involves an "activation" of integrins themselves ("inside-out signaling"), which leads to an increased affinity of the integrin for its ligand that, in turn, largely constitutes an important step in the morphological changes associated with cell spreading on a solid substrate (Disatnik and Rando, 1999). Much relevant to the work reported here, previous studies have indicated that PKC is one of the key intermediates in integrin-dependent signaling in many cell types (Vuori and Ruoslahti, 1993; Lee and Juliano, 2004), particularly through their involvement in both outside-in and inside-out integrin signaling in a positive feedback loop (Disatnik and Rando, 1999). The present results derived from our PKC activation/inhibition analyses indicate that the K8/K18 pair behaves as a modulator of the PKC-mediated integrin-dependent attachment of hepatoma cells, and spreading of both hepatoma cells and hepatocytes, before the induced FAK phosphorylation after integrin engagement (Figure 10). Still, the autophosphorylation of FAK at Tyr-397 creates a binding site for c-Src, which in turn phosphorylates other tyrosine sites in FAK and thereby maximizes c-Src kinase activity and creates additional protein-binding sites (Mitra and Schlaepfer, 2006). For example, an active FAK/c-Src complex mediates the activation of Rho-GTPase effector pathways that act downstream to execute cell adhesion and migration (Huveneers and Danen, 2009).

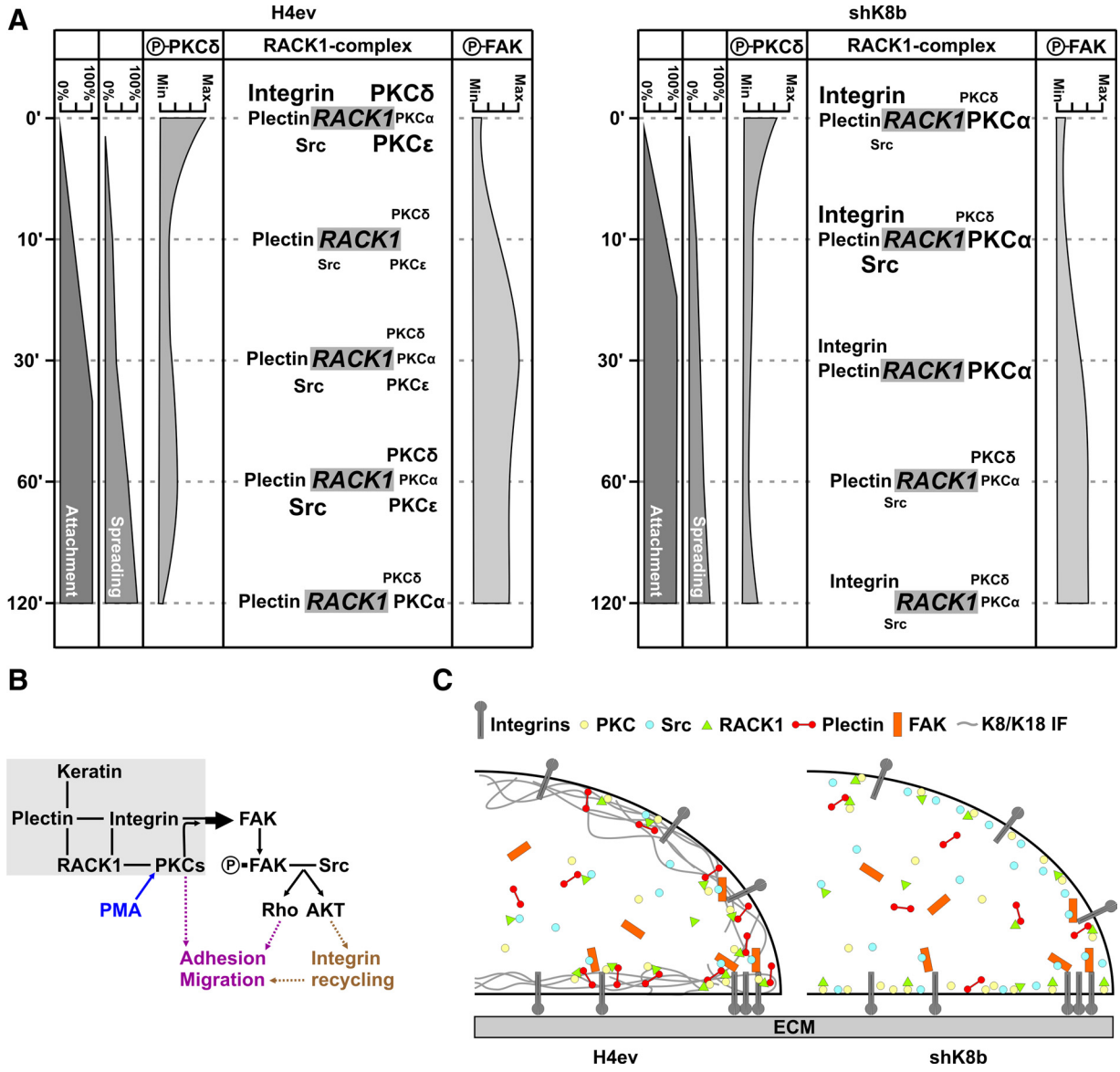

Figure 10. Schematic representations of the integrin/FAK-dependent signaling in adhering and migrating H4ev and shK8b cells. (A) Kinetics of H4ev and shK8b cell attachment and spreading, along with changes in PKC versus FAK phosphorylation and RACK1/β1-integrin/plectin/PKC/c-Src complex assembly. (B) In H4ev cells, the K8/K18 modulation of the integrin/FAK-dependent signaling occurs through a plectin/RACK1/PKC mediation. It involves FAK phosphorylation at Tyr-397 (P-FAK) through a feedback loop, and subsequent activation of downstream c-Src-dependent signaling cascades regulating cell adhesion and migration; note that part of the PKC-mediated migration remains c-Src independent. (C) In light of the immunocomplex and proteome data, a coherent conclusion would be that the K8/K18 loss in shK8b cells leads to a mislocalization of plectin and RACK1, which in turn perturbs their interplay with PKC and integrin related-signaling proteins at FAs.

Of particular note, the present results on the migration of H4ev versus shK8b cells indicate that, although RACK1 binds PKC and c-Src (Mamidipudi *et al.*, 2007), the differential PKC-mediated migration remains in part c-Src independent. Nevertheless, by combining these findings with those derived from our complex formation and colocalization analyses, it seems that K8/K18 IFs are modulating the PKC-mediated inside-out signaling during attachment and also the PKC-mediated outside-in signaling feedback loop during spreading, via an interplay between integrins, RACK1 and plectin (Figure 10, B and C).

A previous report on glioma cell migration has demonstrated that PKCε positively regulates this integrin-dependent cellular process, whereas PKCα plays an opposite role (Besson *et al.*, 2002). But a similar study using renal carcinoma cells suggests instead a PKCδ-dependent mediation (Brenner *et al.*, 2008), suggesting that the PKC isoform selection as mediator of cell migration regulation is cell type dependent. The present results on the inhibition/stimulation and/or knockdown of PKCα, PKCδ, and PKCε suggest a specific PKCδ mediation in the K8/K18 modulation of hepatoma single cell migration, which matches the mediating events of novel PKC during cell spreading. In comparison, the data on PKC stimulation and/or inhibition suggests a conventional PKC mediation during hepatocyte spreading (Table 1).

Vinculin is a key regulator of FA formation, and vinculin-null cells exhibit reduced adhesion to ECM proteins, in-

creased migration, fewer and smaller FAs compared with wild-type cells (Saunders *et al*., 2006; Humphries *et al*., 2007). This contrasts with the present findings that shK8b cells display higher attachment, decreased migration and similar FA size, providing a first indication that the K8/K18-lacking hepatoma cell phenotype does not go through a vinculin involvement. Vinculin is an adaptor protein that exerts its function through interactions with actin and talin, so that the vinculin-talin binding drives the clustering of integrins in cell–matrix adhesions, whereas the vinculin–actin interaction provides the major link of the FA core to the actin–cytoskeleton (Saunders *et al*., 2006; Humphries *et al*., 2007). In epithelial cells, keratins interact with actin through the cytoskeletal linker plectin (Rezniczek *et al*., 2004), implying that any keratin IF perturbation can be transmitted to the actin–cytoskeleton only in an indirect manner. Notably, the present results show that the FA size is not particularly affected by the K8/K18 loss in simple epithelial cells, indicating that K8/K18 IFs, along with plectin and actin, are not modulators of the vinculin-dependent FA formation per se. This observation is in line with the finding that in 3T3 fibroblasts the vinculin-mediated formation of FAs takes place independently of the tensile force exerted by the actomyosin machinery (Humphries *et al*., 2007). However, we have reported recently that in liver epithelial cells, K8/K18 IFs constitute a cytoskeletal network that greatly contributes to the mechanical stress response at FA (Bordeleau *et al*., 2008). Intriguingly, another line of work has revealed that the assembly of K8/K18 into IFs takes place through IF particle precursors that originate from FAs, a dynamic process that implicates talin, and probably vinculin (Windoffer *et al*., 2006). Whether these localized IF formations can modulate the FA dynamics and the signal transduction triggered at $\alpha5/\beta1$ integrin in simple epithelial cells constitute an interesting issue.

FRAP analysis on migrating astrocytoma cells has demonstrated that FAK Tyr-397 autophosphorylation increases specifically the time residency of FAK at FAs but not in the cytoplasm (Hamadi *et al*., 2005). Using the same experimental approach, we show here that the time-residency of FAK at FAs in hepatoma cells compares well with those in other cell types and that a K8/K18 loss results to a reduced FAK residency. Although no definitive explanation can be provided for this difference at this time, it remains that the FAK residency is dependent on multiples interactions with FA structural and signaling components (Hamadi *et al*., 2005). So, assuming that the same molecular mechanisms take place in hepatoma cell FAs, the faster FAK recovery half-time we observe in migrating shK8b cells, which contrasts with the quasi immobility of most vinculin-tagged FAs, emphasizes the signaling function of FAK over a structural role. These data, when combined with those on the FAK phosphorylation kinetics, further indicate that the K8/K18 loss in shK8b cells perturbs FAK activation through a dysfunctional PKCδ activation, which in turn affects FAK time residency, FA disassembly, and cell migration.

Still, the assembly and disassembly of FAs during cell migration requires integrin endocytic internalization and recycling (Roberts *et al*., 2004; Caswell *et al*., 2009). The process involves the ECM stimulation of signaling cascades to modulate integrin internal transport at endosomal compartments, with Akt being among the key signaling components. Actually, after integrin engagement, the FAK/c-Src complex activates Akt through a phosphatidylinositol 3-kinase mediation and in turn, Akt has the ability to act on glycogen synthase kinase-3 and ACAP1 to promote the recycling of integrins (Roberts *et al*., 2004; Li *et al*., 2005). Notably, our previous results have revealed differential Akt activations in spreading H4ev versus shK8b cells and WT versus K8-null hepatocytes that largely parallel the FAK autophosphorylation kinetics (Galarneau *et al*., 2007), with a major overall difference in Akt activation between hepatoma cells and hepatocytes. These differential Akt activations are likely linked to differences in $\alpha5\beta1$-integrin recycling (Figure 10B).

ILK and cav-1 are both scaffold proteins that modulate cell migration, but their respective involvement relies on different molecular mechanisms. For example, ILK and its scaffold-function interacting partners PINCH and parvins are expressed according to a decreasing gradient as differentiating epithelial cells migrate along the crypt–villus axis in the intestine, in association with a decrease in fibronectin deposition (Gagné *et al*., 2010). Moreover, a similar line of work using cultured epidermal keratinocytes has also revealed that the joint expression of ILK and ELMO2 actually promotes cell polarity and directional migration in this cell model (Ho *et al*., 2009). But in contrast, a recent study using targeted ILK-null mouse hepatocytes has shown that the ILK loss does not lead to migration perturbation, but to apoptosis (Gkretsi *et al*., 2007). Thus, whether the differences we report here on the subcellular repartitions of ILK in hepatoma cells and hepatocytes contribute to the observed differential migration remains an appealing issue. With regard to cav-1, this multifunctional protein is involved in the endocytic-mediated recycling of surface receptor proteins (Lanzetti and Di Fiore, 2008; Caswell *et al*., 2009). Of particular note, it is mainly involved in $\beta1$-integrin recycling in migrating intestinal epithelial cells (Vassilieva *et al*., 2008), in line with recent evidence on its key participation in directional migration (Grande-Garcia *et al*., 2007). So, in light of the present data on the dramatic differences in cav-1 subcellular distributions between hepatoma cells and hepatocytes, future work along this line, by using, for example, K8/K18-lacking versus -containing liver epithelial cells, will provide key knowledge on the mechanistic differences between migrating and nonmigrating simple epithelial cells.

Together, the results reported here have significant implications for our understanding of the complex signaling involved in the K8/K18-PKC modulation of integrin/FAK-mediated liver epithelial cell adhesion and migration. In addition, liver cells offer a cell reference for further analyses on the relative contribution of K8/K18 versus the other keratins present in migrating epithelial cells of other lineages, for example in epidermis, where an injury triggers the induction of K6 and K16 (and K17) in keratinocytes at the wound edge, and a K6 loss leads to an enhanced directional migration (Wong and Coulombe, 2003); in this case, one possibility might be a keratin modulation of the ILK/ELMO-mediated promotion. Finally, the results offer a new view on the cytoskeletal IF-related signaling relevant to molecular cell mechanisms by which embryogenesis can proceed and metastatic carcinoma may emerge.

ACKNOWLEDGMENTS

We thank Drs. L. H. Tsai, K. Jacobson, and B. Geiger for generous gifts of GFP-FAK, GFP-paxillin, and GFP-vinculin, respectively. We are grateful to Drs. J. N. Lavoie and J. Huot for their critical reading of the manuscript. This work was supported by grants from Cancer Research Society, Canadian Institutes of Health Research, and Natural Sciences and Engineering Research Council.

REFERENCES

Besson, A., Wilson, T. L., and Yong, V. W. (2002). The anchoring protein RACK1 links protein kinase Cepsilon to integrin beta chains. Requirements for adhesion and motility. J. Biol. Chem. *277*, 22073–22084.

Bordeleau, F., Bessard, J., Sheng, Y., and Marceau, N. (2008). Keratin contribution to cellular mechanical stress response at focal adhesions as assayed by laser tweezers. Biochem. Cell Biol. *86*, 352–359.

Brenner, W., Greber, I., Gudejko-Thiel, J., Beitz, S., Schneider, E., Walenta, S., Peters, K., Unger, R., and Thuroff, J. W. (2008). Migration of renal carcinoma cells is dependent on protein kinase Cdelta via beta1 integrin and focal adhesion kinase. Int. J. Oncol. *32*, 1125–1131.

Buensuceso, C. S., Woodside, D., Huff, J. L., Plopper, G. E., and O'Toole, T. E. (2001). The WD protein Rack1 mediates protein kinase C and integrin-dependent cell migration. J. Cell Sci. *114*, 1691–1698.

Caswell, P. T., Vadrevu, S., and Norman, J. C. (2009). Integrins: masters and slaves of endocytic transport. Nat. Rev. Mol. Cell Biol. *10*, 843–853.

Chang, B. Y., Harte, R. A., and Cartwright, C. A. (2002). RACK 1, a novel substrate for the Src protein-tyrosine kinase. Oncogene *21*, 7619–7629.

Chon, J. H., Vizena, A. D., Rock, B. M., and Chaikof, E. L. (1997). Characterization of single-cell migration using a computer-aided fluorescence time-lapse videomicroscopy system. Anal. Biochem. *252*, 246–254.

Coulombe, P. A., and Omary, M. B. (2002). 'Hard' and 'soft' principles defining the structure, function and regulation of keratin intermediate filaments. Curr. Opin. Cell Biol. *14*, 110–122.

Coulombe, P. A., and Wong, P. (2004). Cytoplasmic intermediate filaments revealed as dynamic and multipurpose scaffolds. Nat. Cell Biol. *6*, 699–706.

Crosnier, C., Stamataki, D., and Lewis, J. (2006). Organizing cell renewal in the intestine: stem cells, signals and combinatorial control. Nat. Rev. Genet. *7*, 349–359.

Disatnik, M. H., and Rando, T. A. (1999). Integrin-mediated muscle cell spreading. The role of protein kinase c in outside-in and inside-out signaling and evidence of integrin cross-talk. J. Biol. Chem. *274*, 32486–32492.

Fuchs, E., and Weber, K. (1994). Intermediate filaments: structure, dynamics, function, and disease. Annu. Rev. Biochem. *63*, 345–382.

Gagné, D., Groulx, J. F., Benoit, Y. D., Basora, N., Herring, E., Vachon, P. H., and Beaulieu, J. F. (2010). Integrin-linked kinase regulates migration and proliferation of human intestinal cells under a fibronectin-dependent mechanism. J. Cell Physiol. *222*, 387–400.

Galarneau, L., Loranger, A., Gilbert, S., and Marceau, N. (2007). Keratins modulate hepatic cell adhesion, size and G1/S transition. Exp. Cell Res. *313*, 179–194.

Geiger, B., Bershadsky, A., Pankov, R., and Yamada, K. M. (2001). Transmembrane crosstalk between the extracellular matrix–cytoskeleton crosstalk. Nat. Rev. Mol. Cell Biol. *2*, 793–805.

Gilbert, S., Loranger, A., Daigle, N., and Marceau, N. (2001). Simple epithelium keratins 8 and 18 provide resistance to Fas-mediated apoptosis. The protection occurs through a receptor-targeting modulation. J. Cell Biol. *154*, 763–773.

Gilbert, S., Loranger, A., and Marceau, N. (2004). Keratins modulate c-Flip/extracellular signal-regulated kinase 1 and 2 antiapoptotic signaling in simple epithelial cells. Mol. Cell. Biol. *24*, 7072–7081.

Gilbert, S., Ruel, A., Loranger, A., and Marceau, N. (2008). Switch in Fas-activated death signaling pathway as result of keratin 8/18-intermediate filament loss. Apoptosis *13*, 1479–1493.

Gkretsi, V., Mars, W. M., Bowen, W. C., Barua, L., Yang, Y., Guo, L., St-Arnaud, R., Dedhar, S., Wu, C., and Michalopoulos, G. K. (2007). Loss of integrin linked kinase from mouse hepatocytes in vitro and in vivo results in apoptosis and hepatitis. Hepatology *45*, 1025–1034.

Glenney, J. R., Jr. (1989). Tyrosine phosphorylation of a 22-kDa protein is correlated with transformation by Rous sarcoma virus. J. Biol. Chem. *264*, 20163–20166.

Goetz, J. G., Joshi, B., Lajoie, P., Strugnell, S. S., Scudamore, T., Kojic, L. D., and Nabi, I. R. (2008). Concerted regulation of focal adhesion dynamics by galectin-3 and tyrosine-phosphorylated caveolin-1. J. Cell Biol. *180*, 1261–1275.

Goodwin, J. S., and Kenworthy, A. K. (2005). Photobleaching approaches to investigate diffusional mobility and trafficking of Ras in living cells. Methods *37*, 154–164.

Grande-Garcia, A., Echarri, A., de Rooij, J., Alderson, N. B., Waterman-Storer, C. M., Valdivielso, J. M., and del Pozo, M. A. (2007). Caveolin-1 regulates cell polarization and directional migration through Src kinase and Rho GTPases. J. Cell Biol. *177*, 683–694.

Green, K. J., Bohringer, M., Gocken, T., and Jones, J. C. (2005). Intermediate filament associated proteins. Adv. Protein Chem. *70*, 143–202.

Hamadi, A., Bouali, M., Dontenwill, M., Stoeckel, H., Takeda, K., and Ronde, P. (2005). Regulation of focal adhesion dynamics and disassembly by phosphorylation of FAK at tyrosine 397. J. Cell Sci. *118*, 4415–4425.

Herrmann, H., Kreplak, L., and Aebi, U. (2004). Isolation, characterization, and in vitro assembly of intermediate filaments. Methods Cell Biol. *78*, 3–24.

Ho, E., Irvine, T., Vilk, G. J., Lajoie, G., Ravichandran, K. S., D'Souza, S. J., and Dagnino, L. (2009). Integrin-linked kinase interactions with ELMO2 modulate cell polarity. Mol. Biol. Cell *20*, 3033–3043.

Humphries, J. D., Wang, P., Streuli, C., Geiger, B., Humphries, M. J., and Ballestrem, C. (2007). Vinculin controls focal adhesion formation by direct interactions with talin and actin. J. Cell Biol. *179*, 1043–1057.

Huveneers, S., and Danen, E. H. (2009). Adhesion signaling—crosstalk between integrins, Src and Rho. J. Cell Sci. *122*, 1059–1069.

Hynes, R. O. (2002). Integrins: bidirectional, allosteric signaling machines. Cell *110*, 673–687.

Joshi, B., *et al*. (2008). Phosphorylated caveolin-1 regulates Rho/ROCK-dependent focal adhesion dynamics and tumor cell migration and invasion. Cancer Res. *68*, 8210–8220.

Ku, N. O., and Omary, M. B. (2006). A disease- and phosphorylation-related nonmechanical function for keratin 8. J. Cell Biol. *174*, 115–125.

Lanzetti, L., and Di Fiore, P. P. (2008). Endocytosis and cancer: an 'insider' network with dangerous liaisons. Traffic *9*, 2011–2021.

Laudanna, C., Mochly-Rosen, D., Liron, T., Constantin, G., and Butcher, E. C. (1998). Evidence of zeta protein kinase C involvement in polymorphonuclear neutrophil integrin-dependent adhesion and chemotaxis. J. Biol. Chem. *273*, 30306–30315.

Lee, J. W., and Juliano, R. (2004). Mitogenic signal transduction by integrin- and growth factor receptor-mediated pathways. Mol. Cells *17*, 188–202.

Li, J., Ballif, B. A., Powelka, A. M., Dai, J., Gygi, S. P., and Hsu, V. W. (2005). Phosphorylation of ACAP1 by Akt regulates the stimulation-dependent recycling of integrin beta1 to control cell migration. Dev. Cell *9*, 663–673.

Liao, J., and Omary, M. B. (1996). 14–3-3 proteins associate with phosphorylated simple epithelial keratins during cell cycle progression and act as a solubility cofactor. J. Cell Biol. *133*, 345–357.

Liliental, J., and Chang, D. D. (1998). Rack1, a receptor for activated protein kinase C, interacts with integrin beta subunit. J. Biol. Chem. *273*, 2379–2383.

Lora, J. M., Rowader, K. E., Soares, L., Giancotti, F., and Zaret, K. S. (1998). Alpha3beta1-integrin as a critical mediator of the hepatic differentiation response to the extracellular matrix. Hepatology *28*, 1095–1104.

Loranger, A., Gilbert, S., Brouard, J. S., Magin, T. M., and Marceau, N. (2006). Keratin 8 modulation of desmoplakin deposition at desmosomes in hepatocytes. Exp. Cell Res. *312*, 4108–4119.

Mamidipudi, V., Dhillon, N. K., Parman, T., Miller, L. D., Lee, K. C., and Cartwright, C. A. (2007). RACK1 inhibits colonic cell growth by regulating Src activity at cell cycle checkpoints. Oncogene *26*, 2914–2924.

Marceau, N., Gilbert, S., and Loranger, A. (2004). Uncovering the roles of intermediate filaments in apoptosis. Methods Cell Biol. *78*, 95–129.

Marceau, N., Loranger, A., Gilbert, S., Daigle, N., and Champetier, S. (2001). Keratin-mediated resistance to stress and apoptosis in simple epithelial cells in relation to health and disease. Biochem. Cell Biol. *79*, 543–555.

Mathew, J., Galarneau, L., Loranger, A., Gilbert, S., and Marceau, N. (2008). Keratin-protein kinase C interaction in reactive oxygen species-induced hepatic cell death through mitochondrial signaling. Free Radic. Biol. Med. *45*, 413–424.

Meng, X. N., *et al*. (2009). Characterisation of fibronectin-mediated FAK signalling pathways in lung cancer cell migration and invasion. Br. J. Cancer *101*, 327–334.

Mitra, S. K., and Schlaepfer, D. D. (2006). Integrin-regulated FAK-Src signaling in normal and cancer cells. Curr. Opin. Cell Biol. *18*, 516–523.

Mizuno, H., Ogura, M., Saito, Y., Sekine, W., Sano, R., Gotou, T., Oku, T., Itoh, S., Katabami, K., and Tsuji, T. (2008). Changes in adhesive and migratory characteristics of hepatocellular carcinoma (HCC) cells induced by expression of alpha3beta1 integrin. Biochim. Biophys. Acta *1780*, 564–570.

Ng, T., Shima, D., Squire, A., Bastiaens, P. I., Gschmeissner, S., Humphries, M. J., and Parker, P. J. (1999). PKCalpha regulates beta1 integrin-dependent cell motility through association and control of integrin traffic. EMBO J. *18*, 3909–3923.

Omary, M. B., Ku, N. O., Strnad, P., and Hanada, S. (2009). Toward unraveling the complexity of simple epithelial keratins in human disease. J. Clin. Invest. *119*, 1794–1805.

Omary, M. B., Ku, N. O., Tao, G. Z., Toivola, D. M., and Liao, J. (2006). "Heads and tails" of intermediate filament phosphorylation: multiple sites and functional insights. Trends Biochem. Sci. *31*, 383–394.

Oshima, R. G., Baribault, H., and Caulin, C. (1996). Oncogenic regulation and function of keratins 8 and 18. Cancer Metastasis Rev. *15*, 445–471.

Osmanagic-Myers, S., Gregor, M., Walko, G., Burgstaller, G., Reipert, S., and Wiche, G. (2006). Plectin-controlled keratin cytoarchitecture affects MAP kinases involved in cellular stress response and migration. J. Cell Biol. *174*, 557–568.

Osmanagic-Myers, S., and Wiche, G. (2004). Plectin-RACK1 (receptor for activated C kinase 1) scaffolding: a novel mechanism to regulate protein kinase C activity. J. Biol. Chem. *279*, 18701–18710.

Parker, P. J., and Murray-Rust, J. (2004). PKC at a glance. J. Cell Sci. *117*, 131–132.

Rezniczek, G. A., Janda, L., and Wiche, G. (2004). Plectin. Methods Cell Biol. *78*, 721–755.

Ridge, K. M., Linz, L., Flitney, F. W., Kuczmarski, E. R., Chou, Y. H., Omary, M. B., Sznajder, J. I., and Goldman, R. D. (2005). Keratin 8 phosphorylation by protein kinase C delta regulates shear stress-mediated disassembly of keratin intermediate filaments in alveolar epithelial cells. J. Biol. Chem. *280*, 30400–30405.

Roberts, M. S., Woods, A. J., Dale, T. C., Van Der Sluijs, P., and Norman, J. C. (2004). Protein kinase B/Akt acts via glycogen synthase kinase 3 to regulate recycling of alpha v beta 3 and alpha 5 beta 1 integrins. Mol. Cell. Biol. *24*, 1505–1515.

Rybin, V. O., Guo, J., Gertsberg, Z., Elouardighi, H., and Steinberg, S. F. (2007). Protein kinase Cepsilon (PKCepsilon) and Src control PKCdelta activation loop phosphorylation in cardiomyocytes. J. Biol. Chem. *282*, 23631–23638.

Saunders, R. M., Holt, M. R., Jennings, L., Sutton, D. H., Barsukov, I. L., Bobkov, A., Liddington, R. C., Adamson, E. A., Dunn, G. A., and Critchley, D. R. (2006). Role of vinculin in regulating focal adhesion turnover. Eur. J. Cell Biol. *85*, 487–500.

Schweizer, J., *et al*. (2006). New consensus nomenclature for mammalian keratins. J. Cell Biol. *174*, 169–174.

Sivaramakrishnan, S., Schneider, J. L., Sitikov, A., Goldman, R. D., and Ridge, K.M. (2009). Shear stress induced reorganization of the keratin intermediate filament network requires phosphorylation by PKC {zeta}. Mol. Biol. Cell *20*, 2755–2765.

Toivola, D. M., Nieminen, M. I., Hesse, M., He, T., Baribault, H., Magin, T. M., Omary, M. B., and Eriksson, J. E. (2001). Disturbances in hepatic cell-cycle regulation in mice with assembly-deficient keratins 8/18. Hepatology *34*, 1174–1183.

Vassilieva, E. V., Gerner-Smidt, K., Ivanov, A. I., and Nusrat, A. (2008). Lipid rafts mediate internalization of beta1-integrin in migrating intestinal epithelial cells. Am. J. Physiol. Gastrointest. Liver Physiol. *295*, G965–G976.

Vomastek, T., Iwanicki, M. P., Schaeffer, H. J., Tarcsafalvi, A., Parsons, J. T., and Weber, M. J. (2007). RACK1 targets the extracellular signal-regulated kinase/mitogen-activated protein kinase pathway to link integrin engagement with focal adhesion disassembly and cell motility. Mol. Cell. Biol. *27*, 8296–8305.

Vuori, K., and Ruoslahti, E. (1993). Activation of protein kinase C precedes alpha 5 beta 1 integrin-mediated cell spreading on fibronectin. J. Biol. Chem. *268*, 21459–21462.

Webb, D. J., Donais, K., Whitmore, L. A., Thomas, S. M., Turner, C. E., Parsons, J. T., and Horwitz, A. F. (2004). FAK-Src signalling through paxillin, ERK and MLCK regulates adhesion disassembly. Nat. Cell Biol. *6*, 154–161.

Windoffer, R., Kolsch, A., Woll, S., and Leube, R. E. (2006). Focal adhesions are hotspots for keratin filament precursor formation. J. Cell Biol. *173*, 341–348.

Wong, P., and Coulombe, P. A. (2003). Loss of keratin 6 (K6) proteins reveals a function for intermediate filaments during wound repair. J. Cell Biol. *163*, 327–337.

Wu, L., *et al*. (2008). Distinct FAK-Src activation events promote alpha5beta1 and alpha4beta1 integrin-stimulated neuroblastoma cell motility. Oncogene *27*, 1439–1448.